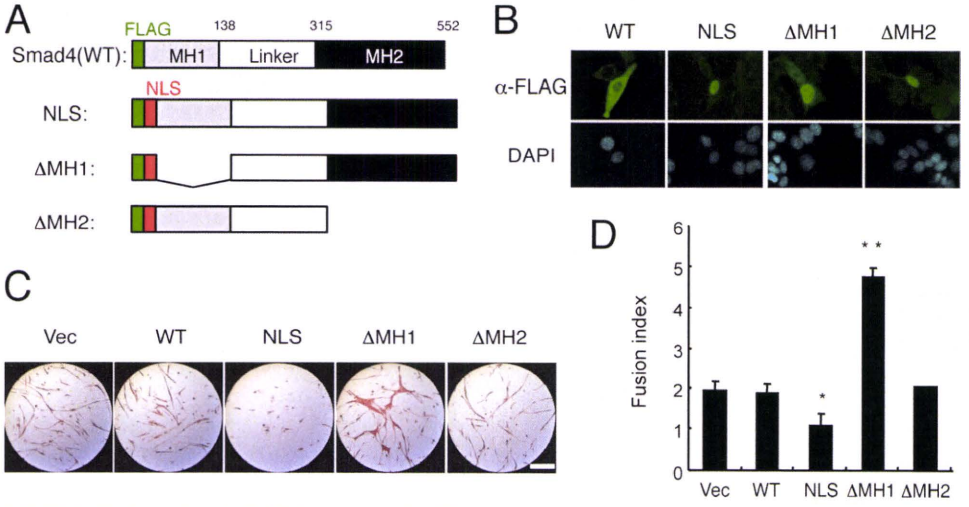

FIGURE 7. **Nuclear Smad4 inhibits myogenic differentiation.** *A*, scheme of construction of FLAG-tagged Smad4 mutants. *B*, cellular localization of FLAG-tagged Smad4 mutants. The cells were immunostained with α-FLAG antibody. *Scale bar*, 25 μm. *C*, effects of Smad4 mutants on myogenic differentiation. C3H10T1/2 cells were co-transfected with *MyoD* and one of the *Smad4* constructs and immunostained for MHC on day 5. *Scale bar*, 400 μm. *D*, fusion index was determined from cultures prepared as in *C*. Values are mean ± S.D. ($n = 3$). *, $p < 0.05$; **, $p < 0.01$. *DAPI*, 4′,6-diamidino-2-phenylindole.

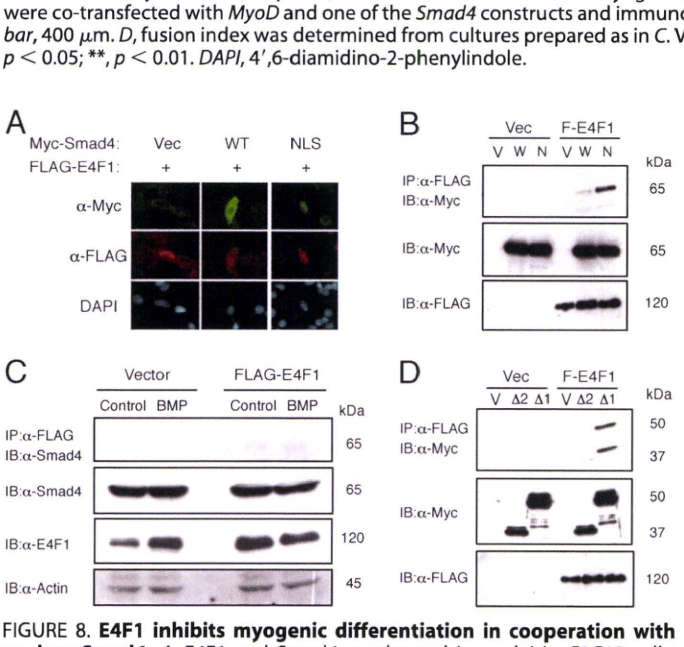

FIGURE 8. **E4F1 inhibits myogenic differentiation in cooperation with nuclear Smad4.** *A*, E4F1 and Smad4 overlapped in nuclei in C2C12 cells. FLAG-tagged *E4F1* and empty vector (*Vec*), *Myc-Smad4* (*WT*), or *Myc-NLS-Smad4* (*NLS*) were cotransfected and stained with α-Myc and α-FLAG antibodies. *B* and *C*, E4F1 interacts with Smad4 *in vivo*. *B*, COS-7 cells were co-transfected with *FLAG-E4F1* and empty vector (*Vec*), *Myc-Smad4* (*WT*), or *Myc-NLS-Smad4* (*NLS*). Whole cell lysates were immunoprecipitated (*IP*) with α-FLAG antibody followed by immunoblotting (*IB*) using α-Myc antibody. *C*, C2C12 cells transfected with *Flag-E4F1* were treated for 1 h without or with 100 ng/ml of BMP-4. Whole cell lysates were immunoprecipitated with M2-agarose beads followed by immunoblotting with antibodies for E4F1, Smad4, and actin. *D*, the MH2 domain of Smad4 is required for interaction with E4F1. The interaction between E4F1 and Smad4 was determined by cotransfection of *Flag-E4F1* and *Myc-NLS-Smad4*(*ΔMH2*) or *Myc-NLS-Smad4*(*ΔMH1*) in COS-7 cells. *DAPI*, 4′,6-diamidino-2-phenylindole.

E4F1 may inhibit myogenesis as a transcription factor rather than as a ubiquitin ligase (Fig. 9*B*). Although *Myogenin* is one of the targets of MyoD and is markedly suppressed by BMP signaling, we could not detect Smad4 or E4F1 binding to the *Myogenin* promoter in response to BMP-4 (supplemental Fig. S2). RNAi knockdown of E4F1 increased the number of MHC-positive C2C12 cells in the presence of BMP signaling (Fig. 9, *D* and *E*). Similar results were obtained using a plasmid-based microRNA expression vector for E4F1 (supplemental Fig. S3). We further examined the role of E4F1 in myogenesis in cell line clone 16 established from *Smad4*$^{floxed/floxed}$ MEFs. Again, deletion of *Smad4* by Cre-adenovirus infection increased the number of MyoD-induced MHC- and myogenin-positive myogenic cells (Fig. 9, *F* and *G*). Co-transfection of *Smad4* and *E4F1* markedly reduced the number of myogenic cells, suggesting that E4F1 acts cooperatively with Smad4 (Fig. 9*F*).

Id1–3 suppress myogenesis and are targets of BMP signaling. Transfection of *E4f1* increased Id1-, Id2-, and Id3-luc activities in C2C12 cells treated with and without BMP-4 (Fig. 9*G*, and data not shown). This stimulation by E4F1 seemed to be Smad4 dependent because the activity was lost by Smad4 ablation and restored by Smad4 overexpression in MEF clone 16 (Fig. 9*G*).

DISCUSSION

In the present study, we examined the molecular mechanisms underlying the conversion of myoblasts by BMPs, allowing their differentiation into osteoblastic cells. It has been suggested that a unique type of intracellular BMP signaling is involved in this conversion, because other inhibitors of myogenic differentiation, such as TGF-β and fibroblast growth factors, do not induce ectopic bone formation *in vivo* or osteoblastic differentiation *in vitro* (12). We found that the inhibition of myogenic differentiation by BMP-4 required treatment for less than 1 h, although induction of osteoblastic differentiation required treatment for more than 9 h. Both activities of BMPs were dependent on the Smad pathway, suggesting that related but distinct mechanisms regulate the conversion of myoblasts into osteoblastic cells. Because we failed to detect cells positive for both MHC and ALP in C2C12 cell cultures treated with BMPs (9, 12), it appeared that osteoblastic differentiation is activated only in immature myoblasts that have not yet initiated myogenic differentiation (34). This hypothesis was confirmed by our preliminary observation that BMPs did not induce ALP activity in mature multinucleated myotubes.[3]

BMP treatment can convert the differentiation pathway of myoblasts into osteoblastic cells and overexpression of constitutively activated BMP type I receptors such as BMPR-IA, BMPR-IB, and ALK2 can have the same effect without requiring the addition of BMPs (35, 36). However, we found that levels of endogenous Smad1 and Smad5 were low in C2C12 cells and that overexpression of wild-type Smad1 was required for induction of osteoblastic differentiation by BMPR-IA(Q233D). These findings suggested that downstream signaling of BMP type I receptors, rather than BMP type II and co-receptors,

[3] J. Nojima, T. Takada, and T. Katagiri, unpublished data.

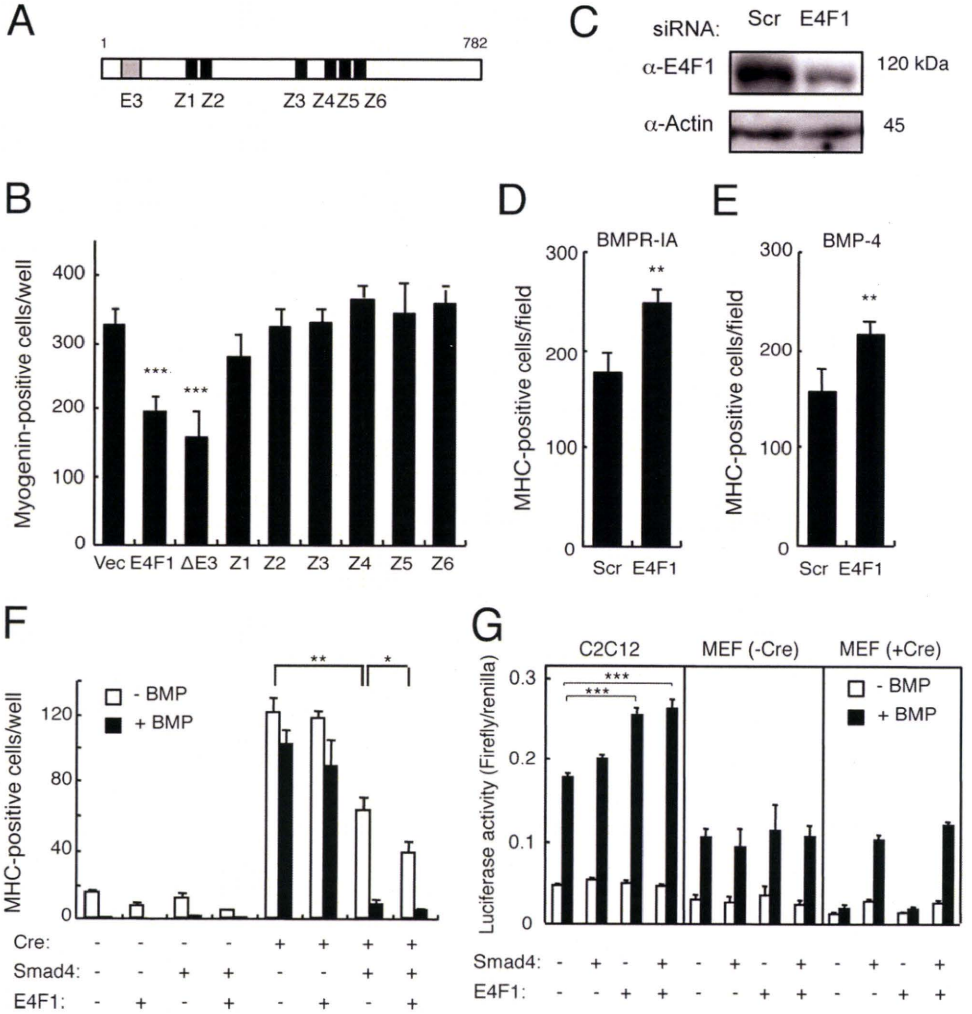

FIGURE 9. **E4F1 is involved in the BMP-induced inhibition of myogenesis.** *A*, schematic structure of E4F1. *E3*, an E3 ubiquitin ligase domain; *Z*, zinc fingers. *B*, overexpression of E4F1 inhibits myogenic differentiation. C3H10T1/2 cells were co-transfected with *MyoD* and wild-type *E4F1*, *E4F1*(*ΔE3*), or a zinc finger mutant *E4F1* and immunostained for myogenin on day 3. Values are mean ± S.D. ($n = 3$). ***, $p < 0.001$. *C*, 20 nmol of *E4F1* siRNA or scrambled oligonucleotide was transfected in C2C12 cells, and protein levels were determined by Western blots at 24 h post-transfection. *D* and *E*, the siRNA-transfected C2C12 cells were co-transfected with *Bmpr-Ia*(*Q233D*) (*D*) or treated with 100 ng/ml of BMP-4 (*E*), and MHC-positive cells were counted on day 5. Values are mean ± S.D. ($n = 3$). **, $p < 0.01$ compared with each scrambled siRNA transfection group. *F*, E4F1 suppresses myogenesis cooperatively with Smad4. *Smad4*$^{floxed/floxed}$-derived clonal cell line 16 was infected with or without a Cre-expressing adenovirus. The cells were transfected with or without *Smad4* in the presence or absence of Smad4, cultured with or without 100 ng/ml of BMP-4, and stained for MHC on day 3. Values are mean ± S.D. ($n = 3$). *, $p < 0.05$; **, $p < 0.01$. *G*, E4F1 stimulates *Id1* expression. C2C12 cells and MEF clone 16 infected with Cre adenovirus were transfected with *Id985-luc*, *E4F1*, and *Smad4* and were then cultured in the presence or absence of 50 ng/ml of BMP-4. Luciferase activity was determined on day 1. Values are mean ± S.D. ($n = 3$). *, $p < 0.05$; **, $p < 0.01$; ***, $p < 0.001$.

plays an important role in the conversion of myoblast differentiation. We established a constitutively activated Smad1, Smad1(DVD), to directly examine the role of the Smad pathway without activation of other signaling pathways induced by BMP receptors, such as the mitogen-activated protein kinase and phosphatidylinositol 3-kinase pathways. Serine residues were substituted with aspartic residues in Smad1(DVD) to introduce negative charges in the SVS motif at the carboxyl terminus, the site of phosphorylation by type I BMP receptors. These substitutions may induce conformational changes and stimulate interaction with coactivators such as p300, OAZ, and Runx2 (11). Indeed, Smad1(DVD) was directly recognized by the α-phospho-Smad1/5/8 antibody, suggesting that its three-dimensional structure is similar to that of native Smad1 phosphorylated by the receptors. We found that co-transfection of *Smad1(DVD)* with *Smad4* was capable of inducing osteoblastic differentiation of C2C12 myoblasts, and this induction was not inhibited by co-expression with Smad7, suggesting that Smad1(DVD) induces activation downstream of BMP type I receptors without activating endogenous BMPs or receptors. However, the ALP activity induced by Smad1(DVD) and Smad4 was lower than that induced by cotransfection of a constitutively activated BMPR-IA receptor and wild-type Smad1, although it was higher than that induced by BMPR-IA(Q233D) alone or Smad1(EVE), in which serine residues had been substituted with glutamic acids instead of aspartic acids.[3] These findings suggested that native phosphorylated Smad1 may have higher affinity for the coactivators required for osteoblastic differentiation than Smad1(DVD) or Smad1(EVE). This hypothesis will require further testing.

The Smad signaling pathway was also involved in the inhibition of myogenic differentiation. In contrast to osteoblast differentiation, however, this inhibitory activity of the Smad pathway appeared to be mainly dependent on Smad4 rather than R-Smads. In particular, the nuclear-targeted Smad4 markedly suppressed myogenic differentiation, although overexpression of NLS-Smad4 did not induce osteoblastic differentiation,[3] suggesting that Smad4 in complex with R-Smads inhibits myogenic differentiation after translocation from the cytoplasm to the nucleus in response to BMP stimulation. Because Smad4 is a common Smad among the TGF-β superfamily members, it may also be involved in mediating the effects of other myogenic inhibitors, such as TGF-βs, myostatin, and activin (37, 38).

The MH1 and MH2 domains of Smads have been shown to be involved in DNA binding and interaction with other proteins, respectively (39). Our deletion analysis suggested that nuclear Smad4 may interact with other transcriptional factor(s) and recruit them to the target DNA sequences via the MH2 and MH1 domains, respectively, to suppress myogenesis. This hypothesis was further supported by the finding of

stimulation of myogenic differentiation by NLS-Smad4(ΔMH1); this mutant Smad4 lacking DNA-binding activity may quench the transcriptional activity of the complex via the MH2 domain. It also appeared that a component of the Smad4 complex, interacting through the MH2 domain, is critical for inhibition of myogenic differentiation in response to BMPs. In the present study, we identified E4F1 as one of the components of the Smad4 complex in the nucleus, interacting through the MH2 domain. E4F1 is a zinc finger DNA-binding protein, identified as a cellular target of viral oncoproteins and shown to regulate the cell cycle (40–42). Our findings indicated that overexpression of E4F1 inhibited myogenic differentiation cooperatively with Smad4. Moreover, RNAi knockdown of E4F1 prevented the inhibition of myogenic differentiation by BMP signaling. Although E4F1 was recently shown to act as a ubiquitin E3 ligase of p53 (43), our findings indicated that deletion of the ubiquitin E3 ligase domain from E4F1 still allowed inhibition of myogenic differentiation. However, all of the zinc finger structures of E4F1 seemed to be important for this inhibitory activity. Taken together, these findings suggest that Smad4, which undergoes nuclear translocation in response to BMP stimulation, may interact with E4F1 in the nucleus to suppress myogenic differentiation as a transcription factor, independent of its ubiquitin E3 ligase activity. Recently, it was reported that Smad4 regulates the processing of pri-microRNA into mature microRNA in response to BMP-2 treatment (44). The direct target gene(s) of the complex still needs to be identified. It is interesting to note that loss-of-function mutations of p53 and Smad4 were identified in some tumors, suggesting that mutations in the Smad4-E4F1-p53 axis might play a role in tumorigenesis (45, 46).

We found that E4F1 stimulated the expression of *Id1–3* in the presence of Smad4. Id proteins inhibit myogenesis and are targets of BMP signaling. Recently, insufficient skeletal muscle repair was reported in $Id1^{+/-}Id3^{-/-}$ mice after muscle injury (47). BMP signaling may also up-regulate *Id* expression in healing muscle tissue (47). Because expression of *Ids* leads to cell cycle progression, the E4F1-induced Ids may suppress myogenic differentiation and maintain myoblast proliferation. Further studies are needed to elucidate the physiological roles of Smads and E4F1 in muscle development and regeneration *in vivo*.

In the present study, we obtained an unexpected finding related to Smads. BMP-induced osteoblastic differentiation was not completely blocked in the *Smad4*-deleted MEFs. There are some possible explanations for this finding: 1) undetectable levels of Smad4 still remained in the MEFs expressing Cre recombinase, 2) an alternative pathway, including a novel Co-Smad, transduced BMP signaling, or 3) Smad4 is not essential for the osteoblastic differentiation induced by BMPs. Recently, evidence has been presented that bone and cartilage tissues were formed during development in the absence of functional Smad4 in mice, although such mice exhibited abnormalities (48). Deletion of *Smad4* in mouse mature osteoblasts using a Cre-loxP system significantly reduced bone volume and osteoblast function *in vivo*, but they still had bone tissues and osteoblasts (48). Further study will be required to elucidate the roles of Smad4 in bone metabolism.

In conclusion, we found that the Smad-dependent pathway regulates both the inhibition of myogenic differentiation and the induction of osteoblastic differentiation induced by BMPs. The introduction of negative charges at the carboxyl terminus of Smad1 may play an important role in the induction of osteoblast differentiation in response to BMPs. In contrast, nuclear Smad4, rather than R-Smad, and E4F1, a novel partner of nuclear Smad4, are responsible for the inhibition of myogenic differentiation by BMPs.

Acknowledgments—We thank Drs. Naoyuki Takahashi, Tatsuo Suda, Ken Yagi, and Masami Muramatsu and members of the Division of Pathophysiology, Research Center for Genomic Medicine, Saitama Medical University, and the Department of Biochemistry, School of Dentistry, Showa University, for valuable comments, discussions, and encouragement. We are grateful to Drs. J. A. Langer, T. Komori, K. Kawakami, and C. Deng for kindly providing constructs, reagents, and mice. We thank Kiyoshiro Imawano for encouragement.

REFERENCES

1. Katagiri, T., Suda, T., and Miyazono, K. (2008) *The Bone Morphogenetic Proteins*, pp. 121–149, Cold Spring Harbor Laboratory, Cold Spring Harbor, NY
2. Urist, M. R. (1965) *Science* **150,** 893–899
3. Wozney, J. M., Rosen, V., Celeste, A. J., Mitsock, L. M., Whitters, M. J., Kriz, R. W., Hewick, R. M., and Wang, E. A. (1988) *Science* **242,** 1528–1534
4. Wozney, J. M., and Rosen, V. (1998) *Clin. Orthop. Relat. Res.* **346,** 26–37
5. Sampath, T. K., Muthukumaran, N., and Reddi, A. H. (1987) *Proc. Natl. Acad. Sci. U.S.A.* **84,** 7109–7113
6. Salminen, A., Braun, T., Buchberger, A., Jürs, S., Winter, B., and Arnold, H. H. (1991) *J. Cell Biol.* **115,** 905–917
7. Yoshida, S., Fujisawa-Sehara, A., Taki, T., Arai, K., and Nabeshima, Y. (1996) *J. Cell Biol.* **132,** 181–193
8. Katagiri, T., Yamaguchi, A., Komaki, M., Abe, E., Takahashi, N., Ikeda, T., Rosen, V., Wozney, J. M., Fujisawa-Sehara, A., and Suda, T. (1994) *J. Cell Biol.* **127,** 1755–1766
9. Massagué, J., Cheifetz, S., Endo, T., and Nadal-Ginard, B. (1986) *Proc. Natl. Acad. Sci. U.S.A.* **83,** 8206–8210
10. Liu, D., Black, B. L., and Derynck, R. (2001) *Genes Dev.* **15,** 2950–2966
11. Miyazono, K., Maeda, S., and Imamura, T. (2005) *Cytokine Growth Factor Rev.* **16,** 251–263
12. Wan, M., and Cao, X. (2005) *Biochem. Biophys. Res. Commun.* **328,** 651–657
13. Katagiri, T., Imada, M., Yanai, T., Suda, T., Takahashi, N., and Kamijo, R. (2002) *Genes Cells* **7,** 949–960
14. Liu, C. J., Ding, B., Wang, H., and Lengyel, P. (2002) *Mol. Cell. Biol.* **22,** 2893–2905
15. López-Rovira, T., Chalaux, E., Massagué, J., Rosa, J. L., and Ventura, F. (2002) *J. Biol. Chem.* **277,** 3176–3185
16. Shore, E. M., Xu, M., Feldman, G. J., Fenstermacher, D. A., Cho, T. J., Choi, I. H., Connor, J. M., Delai, P., Glaser, D. L., LeMerrer, M., Morhart, R., Rogers, J. G., Smith, R., Triffitt, J. T., Urtizberea, J. A., Zasloff, M., Brown, M. A., and Kaplan, F. S. (2006) *Nat. Genet.* **38,** 525–527
17. Fukuda, T., Kohda, M., Kanomata, K., Nojima, J., Nakamura, A., Kamizono, J., Noguchi, Y., Iwakiri, K., Kondo, T., Kurose, J., Endo, K., Awakura, T., Fukushi, J., Nakashima, Y., Chiyonobu, T., Kawara, A., Nishida, Y., Wada, I., Akita, M., Komori, T., Nakayama, K., Nanba, A., Maruki, Y., Yoda, T., Tomoda, H., Yu, P. B., Shore, E. M., Kaplan, F. S., Miyazono, K., Matsuoka, M., Ikebuchi, K., Ohtake, A., Oda, H., Jimi, E., Owan, I., Okazaki, Y., and Katagiri, T. (2009) *J. Biol. Chem.* **284,** 7149–7156
18. Maruyama, Z., Yoshida, C. A., Furuichi, T., Amizuka, N., Ito, M.,

Fukuyama, R., Miyazaki, T., Kitaura, H., Nakamura, K., Fujita, T., Kanatani, N., Moriishi, T., Yamana, K., Liu, W., Kawaguchi, H., Nakamura, K., and Komori, T. (2007) *Dev. Dyn.* **236,** 1876–1890
19. Goldman, L. A., Cutrone, E. C., Kotenko, S. V., Krause, C. D., and Langer, J. A. (1996) *BioTechniques* **21,** 1013–1015
20. Katagiri, T., Akiyama, S., Namiki, M., Komaki, M., Yamaguchi, A., Rosen, V., Wozney, J. M., Fujisawa-Sehara, A., and Suda, T. (1997) *Exp. Cell Res.* **230,** 342–351
21. Yu, P. B., Hong, C. C., Sachidanandan, C., Babitt, J. L., Deng, D. Y., Hoyng, S. A., Lin, H. Y., Bloch, K. D., and Peterson, R. T. (2008) *Nat. Chem. Biol.* **4,** 33–41
22. Yang, X., Li, C., Herrera, P. L., and Deng, C. X. (2002) *Genesis* **32,** 80–81
23. Kanegae, Y., Lee, G., Sato, Y., Tanaka, M., Nakai, M., Sakaki, T., Sugano, S., and Saito, I. (1995) *Nucleic Acids Res.* **23,** 3816–3821
24. Kodaira, K., Imada, M., Goto, M., Tomoyasu, A., Fukuda, T., Kamijo, R., Suda, T., Higashio, K., and Katagiri, T. (2006) *Biochem. Biophys. Res. Commun.* **345,** 1224–1231
25. Ohto, H., Kamada, S., Tago, K., Tominaga, S. I., Ozaki, H., Sato, S., and Kawakami, K. (1999) *Mol. Cell. Biol.* **19,** 6815–6824
26. Suzuki, A., Thies, R. S., Yamaji, N., Song, J. J., Wozney, J. M., Murakami, K., and Ueno, N. (1994) *Proc. Natl. Acad. Sci. U.S.A.* **91,** 10255–10259
27. Kao, K. R., and Elinson, R. P. (1988) *Dev. Biol.* **127,** 64–77
28. Hattori, H., Ishihara, M., Fukuda, T., Suda, T., and Katagiri, T. (2006) *Biochem. Biophys. Res. Commun.* **343,** 1118–1123
29. Zhao, B., Katagiri, T., Toyoda, H., Takada, T., Yanai, T., Fukuda, T., Chung, U. I., Koike, T., Takaoka, K., and Kamijo, R. (2006) *J. Biol. Chem.* **281,** 23246–23253
30. Hanai, J., Chen, L. F., Kanno, T., Ohtani-Fujita, N., Kim, W. Y., Guo, W. H., Imamura, T., Ishidou, Y., Fukuchi, M., Shi, M. J., Stavnezer, J., Kawabata, M., Miyazono, K., and Ito, Y. (1999) *J. Biol. Chem.* **274,** 31577–31582
31. Zhang, Y. W., Yasui, N., Ito, K., Huang, G., Fujii, M., Hanai, J., Nogami, H., Ochi, T., Miyazono, K., and Ito, Y. (2000) *Proc. Natl. Acad. Sci. U.S.A.* **97,** 10549–10554
32. Ito, Y., and Miyazono, K. (2003) *Curr. Opin. Genet. Dev.* **13,** 43–47
33. Suzuki, H., Fukunishi, Y., Kagawa, I., Saito, R., Oda, H., Endo, T., Kondo, S., Bono, H., Okazaki, Y., and Hayashizaki, Y. (2001) *Genome Res.* **11,** 1758–1765
34. Pownall, M. E., Gustafsson, M. K., and Emerson, C. P., Jr. (2002) *Annu. Rev. Cell Dev. Biol.* **18,** 747–783
35. Akiyama, S., Katagiri, T., Namiki, M., Yamaji, N., Yamamoto, N., Miyama, K., Shibuya, H., Ueno, N., Wozney, J. M., and Suda, T. (1997) *Exp. Cell Res.* **235,** 362–369
36. Fujii, M., Takeda, K., Imamura, T., Aoki, H., Sampath, T. K., Enomoto, S., Kawabata, M., Kato, M., Ichijo, H., and Miyazono, K. (1999) *Mol. Biol. Cell* **10,** 3801–3813
37. McPherron, A. C., Lawler, A. M., and Lee, S. J. (1997) *Nature* **387,** 83–90
38. He, L., Vichev, K., Macharia, R., Huang, R., Christ, B., Patel, K., and Amthor, H. (2005) *Anat. Embryol.* **209,** 401–407
39. Massagué, J., and Wotton, D. (2000) *EMBO J.* **19,** 1745–1754
40. Le Cam, L., Lacroix, M., Ciemerych, M. A., Sardet, C., and Sicinski, P. (2004) *Mol. Cell. Biol.* **24,** 6467–6475
41. Rooney, R. J., Rothammer, K., and Fernandes, E. R. (1998) *Nucleic Acids Res.* **26,** 1681–1688
42. Lee, K. A., and Green, M. R. (1987) *EMBO J.* **6,** 1345–1353
43. Le Cam, L., Linares, L. K., Paul, C., Julien, E., Lacroix, M., Hatchi, E., Triboulet, R., Bossis, G., Shmueli, A., Rodriguez, M. S., Coux, O., and Sardet, C. (2006) *Cell* **127,** 775–788
44. Sato, M. M., Nashimoto, M., Katagiri, T., Yawaka, Y., and Tamura, M. (2009) *Biochem. Biophys. Res. Commun.* **383,** 125–129
45. Levine, A. J., Momand, J., and Finlay, C. A. (1991) *Nature* **351,** 453–456
46. Hahn, S. A., Schutte, M., Hoque, A. T., Moskaluk, C. A., da Costa, L. T., Rozenblum, E., Weinstein, C. L., Fischer, A., Yeo, C. J., Hruban, R. H., and Kern, S. E. (1996) *Science* **271,** 350–353
47. Clever, J. L., Sakai, Y., Wang, R. A., and Schneider, D. R. (2010) *Am. J. Physiol. Cell Physiol.* 10.1152/ajpcell.00388.2009
48. Tan, X., Weng, T., Zhang, J., Wang, J., Li, W., Wan, H., Lan, Y., Cheng, X., Hou, N., Liu, H., Ding, J., Lin, F., Yang, R., Gao, X., Chen, D., and Yang, X. (2007) *J. Cell Sci.* **120,** 2162–2170

ORIGINAL ARTICLE

JBMR

Protein Phosphatase Magnesium-Dependent 1A–Mediated Inhibition of BMP Signaling Is Independent of Smad Dephosphorylation

Shoichiro Kokabu,[1,2] Junya Nojima,[1] Kazuhiro Kanomata,[1] Satoshi Ohte,[1] Tetsuya Yoda,[2] Toru Fukuda,[1] and Takenobu Katagiri[1]

[1]Division of Pathophysiology, Research Center for Genomic Medicine, Saitama Medical University, Saitama, Japan
[2]Department of Oral and Maxillofacial Surgery, Faculty of Medicine, Saitama Medical University, Saitama, Japan

ABSTRACT

Phosphorylation of Smad1/5/8 at carboxyl-terminal serine residues by type I receptors activates downstream bone morphogenetic protein (BMP) signaling. Protein phosphatase magnesium-dependent 1A (PPM1A) has been shown to suppress BMP activity by dephosphorylating phospho-Smads. We report here that PPM1A suppresses BMP signaling via a novel mechanism. PPM1A inhibited a constitutively activated Smad1 mutant lacking BMP receptor phosphorylation sites. PPM1A reduced the protein levels not only of Smad1 but also of Smad5 and Smad8. A proteasome inhibitor blocked the inhibitory effects of PPM1A on Smad1, but the Smurf-binding motif in the Smad1 linker region was not involved in this inhibition. The phosphatase activity of PPM1A is essential for inhibition. Taken together, these findings suggest that through the dephosphorylation of unidentified substrate(s), PPM1A inhibits BMP signaling by decreasing Smad protein levels via the proteasome pathway. Moreover, knockdown of endogenous PPM1A stimulated osteoblastic differentiation, suggesting that PPM1A may physiologically suppress BMP signaling via Smads. © 2010 American Society for Bone and Mineral Research. 2010 American Society for Bone and Mineral Research. © 2010 American Society for Bone and Mineral Research.

KEY WORDS: BMP; SMAD; PROTEASOME; PHOSPHATASE; PHOSPHORYLATION

Introduction

Bone morphogenetic proteins (BMPs) induce ectopic bone formation in muscle tissues and osteoblastic differentiation of myoblasts in vitro.[1] BMP signaling is transduced by two different types of transmembrane serine/threonine kinase receptors, termed *type I* and *type II receptors*.[2,3] The BMP-bound type II receptor phosphorylates the type I receptor kinase, and the activated BMP type I receptor, in turn, phosphorylates downstream receptor-regulated Smads (R-Smads), including Smad1, Smad5, and Smad8. Phosphorylated R-Smads form heteromeric complexes with Smad4 and translocate into the nucleus to regulate the transcription of target genes such as *Id1*.[4–6]

Activation of the BMP-regulated Smad pathway may play an important role in patients with fibrodysplasia ossificans progressiva (FOP), an autosomal dominant disorder characterized by heterotopic bone formation in muscle tissues.[7] Recently, several mutations in a BMP type I receptor, activin receptor-like kinase 2 (ALK2), have been identified in FOP patients.[7,8] We found that these mutant ALK2 molecules phosphorylate Smad1/5/8 in the absence of BMPs and activate downstream intracellular signaling pathways that lead to the induction of *Id1* expression.[9] To examine the roles of BMP-regulated Smads, we generated a constitutively active form of Smad1, termed *Smad1(DVD)*, in which the carboxy-terminal serine residues have been substituted by aspartic acids. Evaluation of this mutant revealed that its overexpression induced osteoblastic differentiation of C2C12 myoblasts (Nojima et al., submitted for publication). These findings suggest that phosphorylation of the carboxy termini of Smad1/5/8 by BMP type I receptors plays an important role in BMP-induced bone formation. Moreover, these data suggest that Smad inhibitors may be useful for the treatment of FOP because they may prevent heterotopic bone formation.

BMP signal transduction is negatively regulated at several critical steps. BMP antagonists such as Noggin, Chordin, and DAN family members prevent the binding of BMPs to their receptors in the extracellular space.[10] A pseudoreceptor, BAMBI, acts as a dominant-negative receptor for members of the transforming

Received in original form January 23, 2009; revised form June 9, 2009; accepted July 9, 2009. Published online July 13, 2009.
Address correspondence to: Takenobu Katagiri Division of Pathophysiology, Research Center for Genomic Medicine, Saitama Medical University, 1397-1 Yamane, Hidaka-shi, Saitama 350-1241, Japan. E-mail: katagiri@saitama-med.ac.jp
Journal of Bone and Mineral Research, Vol. 25, No. 3, March 2010, pp 653–660
DOI: 10.1359/jbmr.090736

growth factor β (TGF-β) superfamily on the plasma membrane.[11] Smad6 and Smad7 inhibit the kinase activity of type I receptors by direct interaction in the cytoplasm.[12,13] Smad ubiquitination regulatory factor 1 (Smurf1), a member of the HECT family of E3 ubiquitin ligases, has been found to interact with Smad1 and Smad5 via the PPAY motif in their linker regions, thereby triggering their ubiquitination and degradation.[14]

Recent studies have identified Smad phosphatases and have shed light on the roles of phosphorylation and dephosphorylation at the carboxy-terminal SXS motif in Smads.[15] Protein phosphatase magnesium-dependent 1A (PPM1A) was identified as a serine/threonine phosphatase in the PPM family.[16] PPM1A dephosphorylates the carboxy-terminal SXS motifs in Smad2/3 and Smad1 and suppresses the biologic activities of TGF-β and BMPs.[17,18] In this study, we examined the molecular mechanisms of the inhibitory activity of PPM1A on BMP signaling using Smad1(DVD), a constitutively active form of Smad1. We found that PPM1A inhibited Smad1(DVD) activity even though Smad1(DVD) lacks phosphoserine residues at the carboxy terminus. PPM1A reduced the protein levels of Smad1 via a proteasome-dependent mechanism, and its phosphatase activity was independent of a Smurf consensus sequence in the linker region. Moreover, knockdown of endogenous PPM1A stimulated BMP activity in C2C12 cells, suggesting that the inhibition by PPM1A may play an important role in physiologic BMP signaling in myoblasts.

Materials and Methods

Plasmids

Plasmids encoding wild-type mouse Smad1, Smad1(DVD), Smad4, Smad7, and IdWT4F-luc have been described previously.[6] Smad6 and a Smad6 promoter-luciferase reporter were kindly provided by Dr. Kohei Miyazono of University of Tokyo and Dr. Mitsuyasu Kato of Tsukuba University, respectively.[13,19] Human Smurf1 and PPM1A (Accession Numbers NM_020429 and NM_021003, respectively) were obtained using a standard RT-PCR technique employing Platinum Pfx DNA polymerase (Invitrogen, Carlsbad, CA, USA) and cloned into a pcDEF3 expression vector.[20] The Smad1 mutants, Smad1(AAAY-WT) and Smad1(AAAY-DVD), were generated from wild-type Smad1 and Smad1(DVD), respectively, by replacing proline 224 and proline 225 with alanine using a set of mutated PCR primers. A phosphatase activity-deficient PPM1A, PPM1A(R174G/D239N), was generated from wild-type PPM1A by replacing arginine 174 and aspartic acid 239 with glycine and asparagine, respectively, using sets of mutated PCR primers. All the final constructs were confirmed by sequencing.

Cell culture and transfection

C2C12 mouse myoblasts were maintained, treated with 100 ng/mL BMP-4 (R&D Systems, Minneapolis, MN, USA), and transfected with plasmids using Lipofectamine 2000 (Invitrogen) as described previously.[6,21] Cells were treated with 10 μM Lactacystin (Calbiochem, San Diego, CA, USA). Primary osteoblasts were prepared by sequential collagenase digestion of newborn mouse calvaria as described previously.[22]

Luciferase assays

Luciferase assays were performed using IdWT4F-luc, Smad6 promoter-luc, and phRL-SV40 (Promega, Madison, WI, USA) with the Dual-Glo Luciferase Assay System (Promega) as described previously.[6]

Immunohistochemistry and Western blot analysis

The following antibodies were used for immunohistochemistry and Western blot analysis: α-FLAG antibody (clone M2, Sigma Aldrich Chemicals, St. Louis, MO, USA), α-Myc polyclonal antibody (Medical & Biological Laboratories Co., Nagoya, Japan), and α-PPM1A mouse monoclonal antibody (Abcam, Cambridge, MA, USA). For immunohistochemical analysis, target proteins were visualized using an Alexa488- or Alexa594-conjugated secondary antibody (Invitrogen). For Western blot analysis, the target proteins were detected using a horseradish peroxidase–conjugated anti-mouse or anti-rabbit IgG antibody (GE Healthcare UK, Ltd., Buckinghamshire, England).

Reverse-transcriptase PCR and real-time PCR analysis

Total RNA was isolated from C2C12 cells using Trizol (Invitrogen) and then reverse transcribed into cDNA. cDNA was amplified by PCR using primers that were specific for murine *Id1*, *Osterix (Osx)*, *Runx2*, and *GAPDH*, which was used as a control (QIAGEN, Hilden, Germany). SYBR Green-based real-time PCR was performed in a 96-well plate format using SYBR Premix Ex Taq (TaKaRa, Ohtsu, Japan) on an iCycler Thermal Cycler (Bio-Rad, Richmond, CA, USA).

RNAi design and transfection

RNAi Stealth oligonucleotides were designed against murine PPM1A (No. MSS207887, Invitrogen), and a scrambled RNAi was used as a negative control (Invitrogen). Cells were transfected with the RNAi Stealth oligonucleotides using Lipofectamine 2000 according to the manufacturer's instructions (Invitrogen).

Statistical analysis

Comparisons were made using unpaired Student's *t* test. Results are presented as means ± SD. Statistical significance is displayed as $^{*}p < .05$ or $^{**}p < .01$.

Results

PPM1A inhibits BMP signaling induced by a constitutively active Smad1

First, we compared the effect of PPM1A with that of Smad7 and Smurf1 on osteoblastic differentiation of C2C12 myoblasts as induced by treatments with BMP-4, overexpression of a constitutively active ALK2(Q207D) receptor, or overexpression of a constitutively active Smad1(DVD). ALP activity was measured as a typical marker of osteoblastic differentiation. ALP activity induced by BMP-4 or ALK2(Q207D) was suppressed by Smad7 and Smurf1. As reported previously, although Smad6 also suppressed the ALP activity induced by ALK2(Q207D), it was

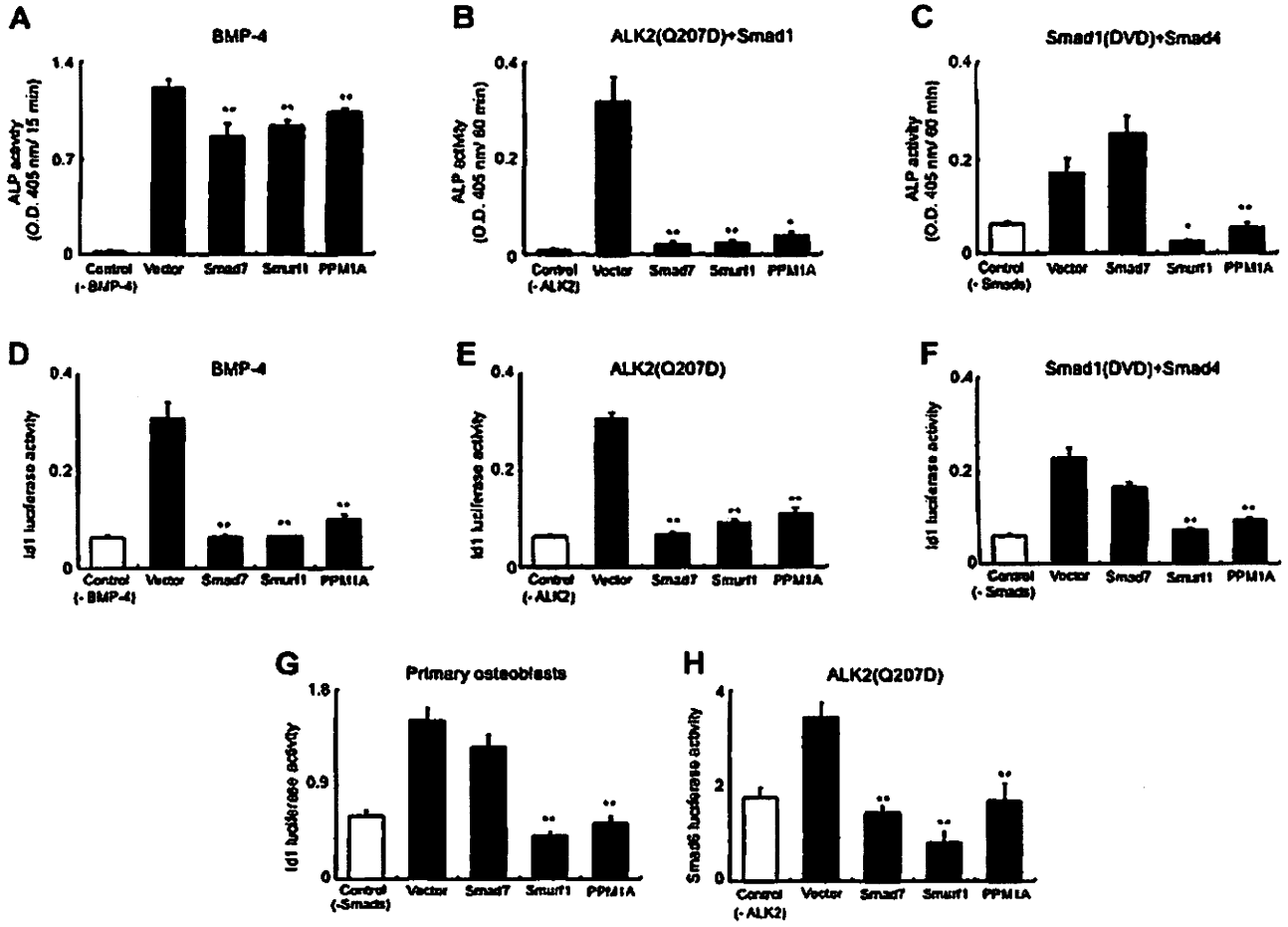

Fig. 1. PPM1A inhibits BMP signaling induced by constitutively active Smad1. (*A–C*) Inhibition of ALP activity by Smad7, Smurf1, and PPM1A in C2C12 cells. ALP activity was induced by BMP-4 treatment (*A*), overexpression of ALK2(Q207D) with wild-type Smad1 (*B*), and overexpression of Smad1(DVD) with Smad4 (*C*). (*D–F*) Inhibition of IdWT4F-luc activity by Smad7, Smurf1, and PPM1A in C2C12 cells. IdWT4F-luc activity was induced by BMP-4 treatment (*D*), overexpression of ALK2(Q207D) (*E*), and overexpression of Smad1(DVD) with Smad4 (*F*). (*G*) Inhibition of IdWT4F-luc activity by Smad7, Smurf1, and PPM1A in primary osteoblasts. IdWT4F-luc activity was induced by overexpression of Smad1(DVD) with Smad4. (*H*) Inhibition of Smad6 promoter-luc activity by Smad7, Smurf1, and PPM1A in C2C12 cells. ALP activity was induced by overexpression of ALK2(Q207D) with wild-type Smad1. Data are presented as means ± SD ($n = 3$). $^{*}p < .05$; $^{**}p < .01$ compared with empty vector transfection in each group.

weaker than Smad7 (data not shown).[9,23] Unexpectedly, ALP suppression likewise was detected in cultures transfected with Smad1(DVD), which lacked serine residues at the carboxy terminus (Fig. 1*A–C*). Next, we examined the inhibitory effect of PPM1A on Smad1 using IdWT4F-luc, which contained the Smad-binding element from the *ID1* gene. PPM1A suppressed the luciferase activity that was induced not only by the ligand and receptor but also by Smad1(DVD) (see Fig. 1*D–F*). A similar suppression by PPM1A was observed in primary osteoblasts (see Fig. 1*G*). PPM1A suppressed not only Id1 promoter activity but also Smad6 promoter-luc activity in C2C12 cells (see Fig. 1*H*).

PPM1A decreases Smad protein levels via the proteasome pathway

Next, we examined the effect of PPM1A on Smad1(DVD) protein levels in C2C12 cells. The number of Smad1(DVD)-positive cells and the protein level of Smad1(DVD), as determined by Western blot analysis, were reduced by coexpression of PPM1A (Fig. 2*A, B*). Protein levels of wild-type Smad1, Smad5, and Smad8 also were reduced by PPM1A expression (see Fig. 2*C*).

Because the proteasome pathway plays a key role in Smad degradation,[24,25] we examined whether this pathway is also involved in the action of PPM1A. Treatment of C2C12 cells with lactacystin, which is a specific inhibitor of the proteasome, increased the number of cells that were positive for both Smad1 and PPM1A and prevented a decrease in Smad1 protein levels (Fig. 3*A, B*). Lactacystin also reduced the inhibitory activity of PPM1A on IdWT4F-luc activity that was induced by Smad1(DVD) (see Fig. 3*C*).

PPM1A decreases Smad1 protein levels independent of a Smurf1 consensus sequence

Smurf1 is a Smad ubiquitin ligase that stimulates Smad degradation via a proteasome pathway by interacting with a conserved PPAY motif in the linker regions of Smads.[14,26,27] Because substitution of the PPAY motif with AAAY destroys the

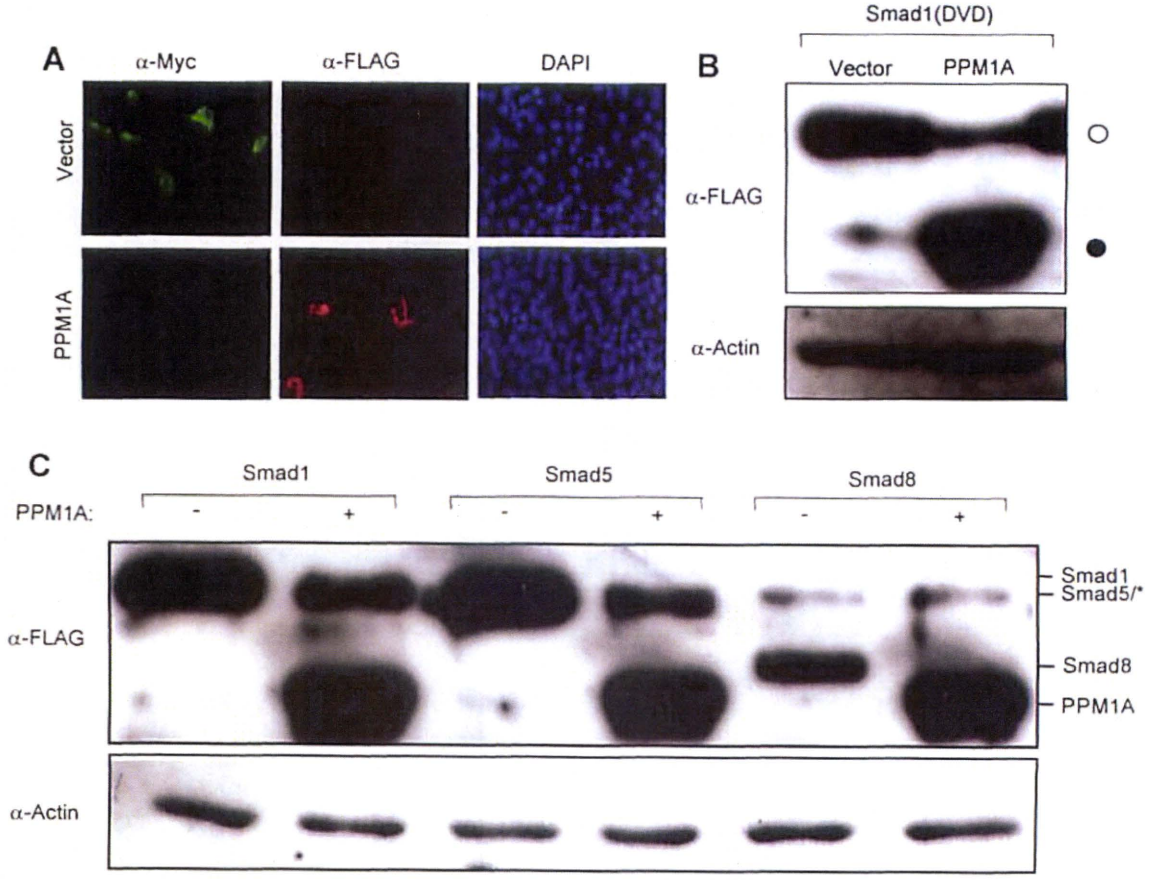

Fig. 2. PPM1A decreases protein levels of Smad1, Smad5, and Smad8 in C2C12 cells. (*A*) C2C12 cells were cotransfected with Myc-Smad1(DVD) and FLAG-PPM1A or with an empty vector, followed by immunohistochemical analysis on day 3 after transfection. Original magnification ×40. (*B*) C2C12 cells were cotransfected with FLAG-tagged Smad1(DVD) (*open circle*) and FLAG-PPM1A (*closed circle*) or an empty vector and analyzed by Western blotting on day 3 after transfection. (*C*) Effects of PPM1A on Smad1, Smad5, and Smad8. C2C12 cells were cotransfected with Smad1, Smad5, or Smad8 along with FLAG-PPM1A or with an empty vector. The cells then were analyzed by Western blotting on day 3 after transfection. Lanes for Smad8 contained nonspecific faint bands (*) with the same mobility as Smad5.

above-mentioned interaction, we introduced this mutation into wild-type Smad1 and Smad1(DVD), which we labeled Smad1(AAAY-WT) and Smad1(AAAY-DVD), respectively. Coexpression of PPM1A with Smad1(AAAY-WT) or Smad1(AAAY-DVD) reduced the protein levels of both types of Smad1 (Fig. 4*A*, *B*). This reduction was confirmed by immunohistochemical analysis of C2C12 cells (unpublished data). Moreover, PPM1A expression almost completely suppressed Smad1(AAAY-DVD)-induced IdWT4F-luc activity (see Fig. 4*C*). Taken together, these findings suggest that the interaction between Smurf1 and Smad1 via the PPAY motif is not involved in the inhibitory action of PPM1A.

Phosphatase activity is necessary for the inhibition of BMP signaling by PPM1A

To determine whether phosphatase activity is required for the action of PPM1A on Smads, we generated a phosphatase activity–deficient version of PPM1A (D239N/R174G).[28] In contrast to wild-type PPM1A, the mutant PPM1A did not suppress the IdWT4F-luc activity induced by BMP-4 or Smad1(DVD) (Fig. 5*A*, *B*). Moreover, mutant PPM1A did not decrease the number of Smad1-positive cells or the Smad1 protein level in C2C12 cells (see Fig. 5*C*, *D*). These findings indicate that the phosphatase activity of PPM1A is necessary for the inhibition of BMP signaling. They also suggest that a molecule(s) other than the Smads may be dephosphorylated by PPM1A.

Knockdown of endogenous PPM1A enhances BMP signaling

Finally, we examined the role of endogenous PPM1A on BMP signaling in C2C12 cells using RNAi (Fig. 6*A*). Transfection of C2C12 cells with siRNA specific for PPM1A efficiently reduced the levels of endogenous PPM1A protein and increased the IdWT4F-luc activity induced by Smad1(DVD) (see Fig. 6*A*, *B*). Moreover, the induction of Id1, Osx, and Runx2 mRNA levels by Smad1(DVD) with Smad4 or BMP-4 was increased by PPM1A-specific siRNA transfection, suggesting that endogenous PPM1A physiologically suppresses osteoblastic differentiation via Smads in C2C12 cells (see Fig. 6*C*–*H*).

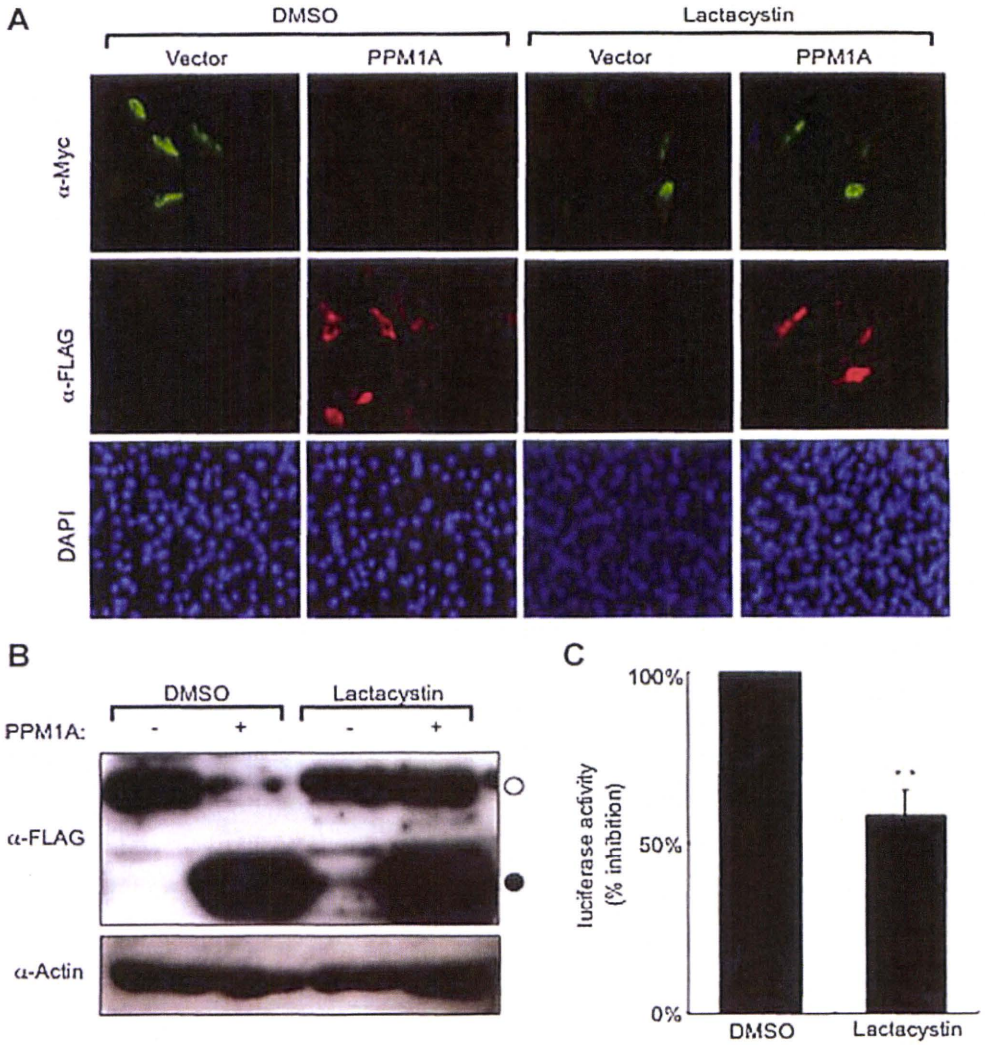

Fig. 3. The proteasome inhibitor lactacystin prevents the inhibitory activity of PPM1A on Smad1. (*A*) Immunohistochemical analysis of Myc-Smad1 and FLAG-PPM1A in C2C12 cells incubated with and without 10 μM lactacystin. Original magnification ×40. (*B*) Western blot analysis of FLAG-Smad1 (*open circle*) and FLAG-PPM1A (*closed circle*) in C2C12 cells incubated with and without 10 μM lactacystin. (*C*) Effect of lactacystin on Id1-luc activity, which is suppressed by PPM1A. C2C12 cells were transfected with IdWT4F-luc and PPM1A and treated with 10 μM lactacystin or vehicle (DMSO) for 8 hours. Data are expressed as percent inhibition relative to the vehicle control. Data are presented as means ± SD ($n = 3$). $^{**}p < .01$.

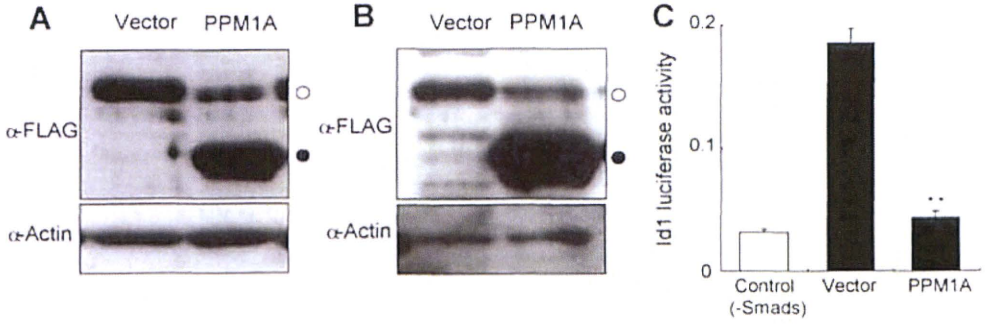

Fig. 4. PPM1A suppresses the activity of Smad1 carrying a mutation in the PPAY motif in the linker region. (*A, B*) C2C12 cells were cotransfected with FLAG-Smad1(AAAY-WT) (*open circle*) (A) or FLAG-Smad1(AAAY-DVD) (*open circle*) (*B*) along with FLAG-PPM1A (*closed circles*) or with an empty vector alone. Cells were analyzed by Western blotting on day 3 after transfection. (*C*) C2C12 cells were cotransfected with Smad1(AAAY-DVD), IdWT4F-luc, and PPM1A expression vector or an empty vector. Luciferase activity was analyzed on day 3 after transfection. Data are presented as means ± SD ($n = 3$). $^{**}p < .01$.

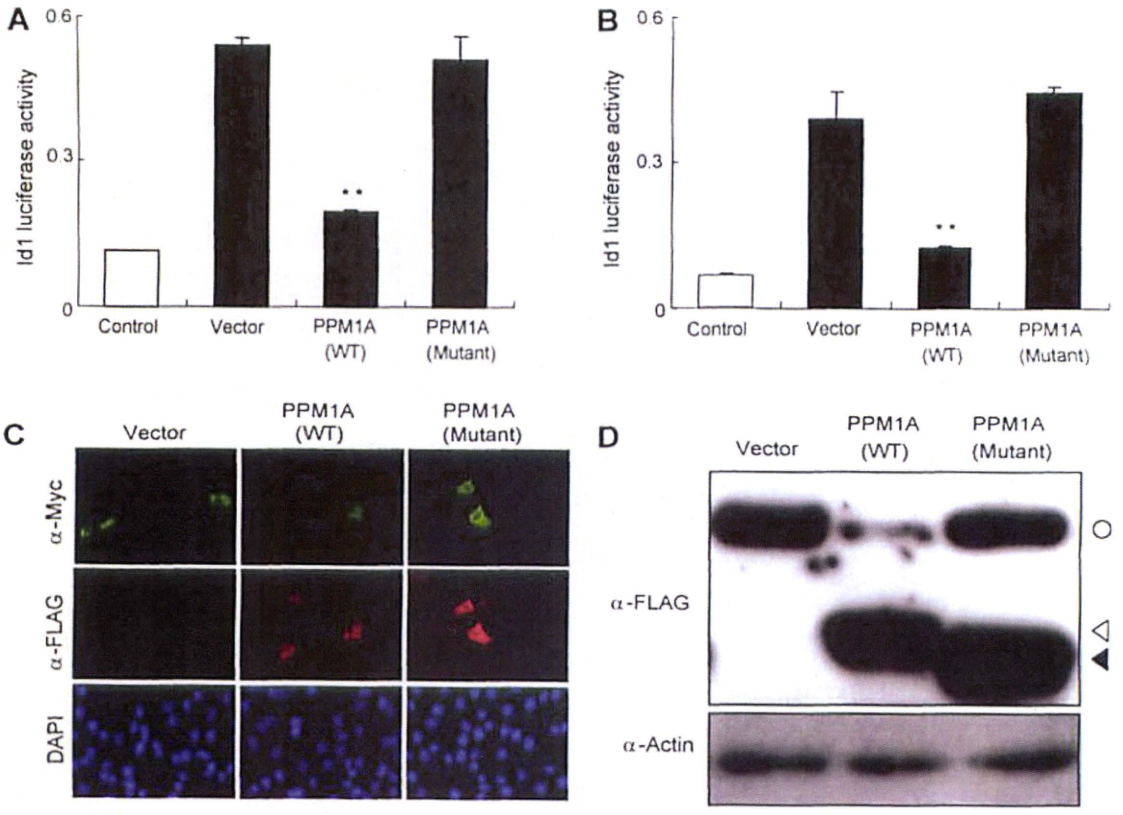

Fig. 5. The phosphatase activity of PPM1A is essential for Smad1 inhibition. (*A, B*) Suppression of IdWT4F-luc activity induced by treatment with BMP-4 (*A*) or by overexpression of Smad1(DVD) (*B*) via wild-type or mutant PPM1A. Data are presented as means ± SD ($n = 3$). $^{**}p < .01$. (*C*) C2C12 cells were cotransfected with Myc-Smad1 and wild-type FLAG-PPM1A, FLAG-PPM1A(R174G/D239N), or empty vector. The cells were submitted to immunohistochemical analysis on day 3 after transfection. Original magnification ×40. (*D*) C2C12 cells were cotransfected with FLAG-Smad1 (*open circle*) and wild-type FLAG-PPM1A (*open triangle*), FLAG-PPM1A(R174G/D239N) (*closed triangle*), or empty vector, followed by Western blot analysis on day 3 after transfection.

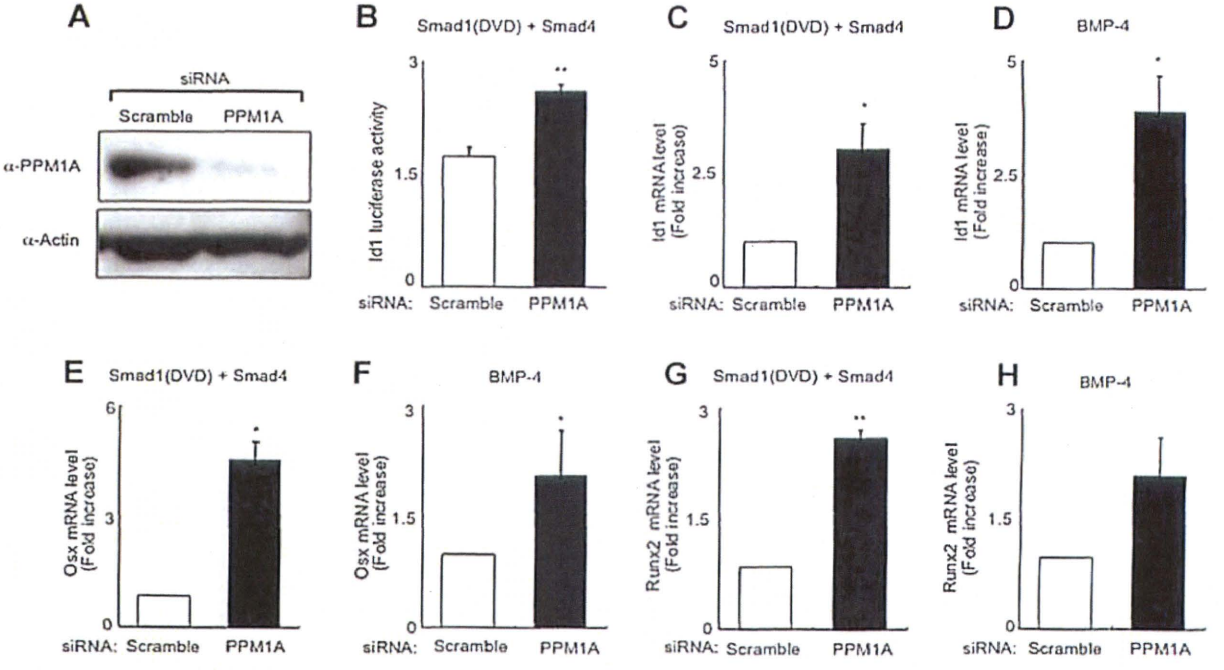

Fig. 6. Knockdown of endogenous PPM1A enhances BMP signaling in C2C12 cells. (*A*) C2C12 cells were transfected with 20 nM PPM1A RNAi or scrambled RNAi. The levels of PPM1A were examined by Western blotting at 24 hours after transfection. (*B*) Transfection of 20 nM PPM1A RNAi stimulated the IdWT4F1-luc activity induced by Smad1(DVD). (*C–H*) Real-time PCR analysis of Id1 (*C, D*), Osx (*E, F*), and Runx2 (*G, H*) mRNA levels in C2C12 cells. Twenty nanomoles of PPM1A siRNA or scrambled oligonucleotide was transfected, and BMP signaling was induced by Smad1(DVD) with Smad4 (*C, E, G*) or BMP-4 (*D, F, H*). Results are presented as means ± SD ($n = 3$). $^{*}p < .05$, $^{**}p < .01$ compared with scrambled RNAi transfection in each group.

Discussion

Type I BMP receptors phosphorylate the carboxy-terminal serine residues of Smad1/5/8 and thereby activate the transcriptional activity of Smads. Importantly, substitution of a phosphorylatable amino acid with an acidic residue (such as aspartic acid or glutamic acid) mimics the phosphorylated state of some proteins, including type I receptors of the TGF-β superfamily. Recently, we found that substitution of the two carboxy-terminal serine residues in Smad1 with aspartic acid residues induced osteoblastic differentiation via constitutive activation of Smad1 (Nojima et al., submitted for publication). Similar mutations at the carboxy-terminal phosphorylation sites of Smad3 have been shown to induce active trimer complex formation.[29] These constitutively activated Smads are useful for examining the role of PPM1A because they activate intracellular signaling just as the receptor-phosphorylated wild-type Smads do, but they are not sensitive to phosphatases targeting their carboxy termini.

In this study we have shown that the phosphatase PPM1A suppresses the induction of BMP signaling by Smad1 even when Smad1's carboxy terminus cannot be dephosphorylated. This finding suggests that PPM1A suppresses BMP signaling via a novel mechanism. Our data suggest that suppression by PPM1A depends on its phosphatase activity through a proteasome pathway. Moreover, we found that knockdown of endogenous PPM1A enhanced BMP activity. Although PPM1A suppressed the BMP signaling of an AAAY mutant, we cannot rule out the possibility that Smurf1 is still involved in the inhibition through interactions with I-Smads or other Smad-interacting molecules. The identification of novel endogenous substrates of PPM1A may help to elucidate the mechanism(s) by which PPM1A inhibits BMP signaling.

In addition to PPM1A, small C-terminal-domain phosphatases (SCPs) have been identified as Smad phosphatases.[30] In our preliminary experiments, SCP1 showed a much weaker inhibitory activity toward Smad1(DVD) than PPM1A, suggesting that dephosphorylation at the carboxy terminus of Smad1 is critical for its suppression by SCP1. Phosphorylation of the linker region by mitogen-activated kinases (MAPKs) inhibited Smad1 activity.[31,32] SCP1 has been shown to dephosphorylate Smad1 not only at its carboxy terminus but also at its linker region.[15] To investigate further, we generated additional Smad1 mutants lacking the ERK and GSK3β phosphorylation sites in the linker region. Similarly to wild type and the AAAY mutant, the ALP activity induced by these mutants was suppressed by PPM1A and SCP1 (data not shown). Further studies are needed to elucidate the molecular mechanisms of PPM1A- and SCP1-dependent inhibition of BMP signaling.

At present, no effective treatment is available to prevent heterotopic bone formation in FOP. A possible cause of this condition is constitutive activation of Smad pathways by the BMP receptor ALK2.[9,33] We have shown that a specific chemical inhibitor of the Smad pathway blocks the biologic activities of mutant ALK2, which is normally found in FOP patients.[9,33] These finding suggest that activation of Smad1/5 by phosphorylation may play an important role in heterotopic bone formation and that Smads should be evaluated as potential targets for novel FOP therapies. Because PPM1A inhibits Smad activity, a stimulator of PPM1A expression in muscle tissues may prevent heterotopic bone formation in FOP.

In conclusion, we have found that PPM1A suppresses BMP signaling by reducing the protein levels of Smad via a proteasome pathway. Thus PPM1A may indirectly regulate BMP signaling by dephosphorylating molecule(s) other than Smads.

Disclosures

The authors state that they have no conflicts of interest.

Acknowledgments

We thank members of the Division of Pathophysiology, Research Center for Genomic Medicine, Saitama Medical University, for their valuable comments and discussion. We are grateful to Drs K Miyazono, M Kato, and JA Langer for kindly providing us with Smad6, Smad6 promoter reporter, and pcDEF3, respectively. This work was supported in part by Health and Labor Sciences Research Grants for Research on Measures for Intractable Research from the Ministry of Health, Labour and Welfare of Japan, a grant-in-aid from the Ministry of Education, Culture, Sports, Science, and Technology of Japan, a grant-in-aid from the Sankyo Foundation of Life Science, a grant-in-aid from the Kawano Masanori Memorial Foundation for Promotion of Pediatrics, a grant-in-aid from the Novo Nordisk Award for Growth and Development, a grant-in-aid from the Takeda Science Foundation, and a grant-in-aid from the Support Project for the Formation of Strategic Center in Private University from the Ministry of Education, Culture, Sports, Science and Technology of Japan. SK is a recipient of the Saitama Medical University Research Fellowship.

References

1. Katagiri T, Suda T, Miyazono K. The bone morphogenetic proteins. In: Derynck R, Miyazono K, eds. *The TGF-β Family*. Cold Spring Harbor, NY: Cold Spring Harbor Press, 2008:121–149.
2. Wan M, Cao X. BMP signaling in skeletal development. Biochem Biophys Res Commun 2005;328:651–657.
3. Miyazono K, Maeda S, Imamura T. BMP receptor signaling: transcriptional targets, regulation of signals, and signaling cross-talk. Cytokine Growth Factor Rev 2005;16:251–263.
4. Lopez-Rovira T, Chalaux E, Massague J, Rosa JL, Ventura F. Direct binding of Smad1 and Smad4 to two distinct motifs mediates bone morphogenetic protein-specific transcriptional activation of *Id1* gene. J Biol Chem 2002;277:3176–3185.
5. Liu CJ, Ding B, Wang H, Lengyel P. The MyoD-inducible p204 protein overcomes the inhibition of myoblast differentiation by Id proteins. Mol Cell Biol 2002;22:2893–2905.
6. Katagiri T, Imada M, Yanai T, Suda T, Takahashi N, Kamijo R. Identification of a BMP-responsive element in *Id1*, the gene for inhibition of myogenesis. Genes Cells 2002;7:949–960.
7. Kaplan FS, Xu M, Seemann P, et al. Classic and atypical fibrodysplasia ossificans progressiva (FOP) phenotypes are caused by mutations in the bone morphogenetic protein (BMP) type I receptor ACVR1. Hum Mutat. 2009;30:379–390.

8. Shore EM, Xu M, Feldman GJ, et al. A recurrent mutation in the BMP type I receptor ACVR1 causes inherited and sporadic fibrodysplasia ossificans progressiva. Nat Genet 2006;38:525–527.
9. Fukuda T, Kohda M, Kanomata K, et al. Constitutively activated ALK2 and increased Smad1/5 cooperatively induce BMP signaling in fibrodysplasia ossificans progressiva. J Biol Chem. 2009;284:7149–7156.
10. Balemans W, Van Hul W. Extracellular regulation of BMP signaling in vertebrates: a cocktail of modulators. Dev Biol 2002;250:231–250.
11. Onichtchouk D, Chen YG, Dosch R, et al. Silencing of TGF-β signalling by the pseudoreceptor BAMBI. Nature 1999;401:480–485.
12. Nakao A, Afrakhte M, Moren A, et al. Identification of Smad7, a TGF-β-inducible antagonist of TGF-β signalling. Nature 1997;389:631–635.
13. Imamura T, Takase M, Nishihara A, et al. Smad6 inhibits signalling by the TGF-β superfamily. Nature 1997;389:622–626.
14. Zhu H, Kavsak P, Abdollah S, Wrana JL, Thomsen GH. A SMAD ubiquitin ligase targets the BMP pathway and affects embryonic pattern formation. Nature 1999;400:687–693.
15. Sapkota G, Knockaert M, Alarcon C, Montalvo E, Brivanlou AH, Massague J. Dephosphorylation of the linker regions of Smad1 and Smad2/3 by small C-terminal domain phosphatases has distinct outcomes for bone morphogenetic protein and transforming growth factor-β pathways. J Biol Chem 2006;281:40412–40419.
16. Tamura S, Li G, Komaki K, Sasaki M, Kobayashi T. Roles of mammalian protein phosphatase 2C family members in the regulation of cellular functions. In: Alexander JAaDR, ed. *Protein Phosphatases*. Heidelberg: Springer-Verlag, 2003:91–105.
17. Duan X, Liang YY, Feng XH, Lin X. Protein serine/threonine phosphatase PPM1A dephosphorylates Smad1 in the bone morphogenetic protein signaling pathway. J Biol Chem 2006;281:36526–36532.
18. Lin X, Duan X, Liang YY, et al. PPM1A functions as a Smad phosphatase to terminate TGFβ signaling. Cell 2006;125:915–928.
19. Ishida W, Hamamoto T, Kusanagi K, et al. Smad6 is a Smad1/5-induced Smad inhibitor: characterization of bone morphogenetic protein-responsive element in the mouse Smad6 promoter. J Biol Chem 2000;275:6075–6079.
20. Goldman LA, Cutrone EC, Kotenko SV, Krause CD, Langer JA. Modifications of vectors pEF-BOS, pcDNA1 and pcDNA3 result in improved convenience and expression. Biotechniques 1996;21:1013–1015.
21. Katagiri T, Yamaguchi A, Komaki M, et al. Bone morphogenetic protein-2 converts the differentiation pathway of C2C12 myoblasts into the osteoblast lineage. J Cell Biol 1994;127:1755–1766.
22. Komaki M, Katagiri T, Suda T. Bone morphogenetic protein-2 does not alter the differentiation pathway of committed progenitors of osteoblasts and chondroblasts. Cell Tissue Res 1996;284:9–17.
23. Goto K, Kamiya Y, Imamura T, Miyazono K, Miyazawa K. Selective inhibitory effects of Smad6 on bone morphogenetic protein type I receptors. J Biol Chem 2007;282:20603–20611.
24. Hershko A, Ciechanover A. The ubiquitin system. Annu Rev Biochem 1998;67:425–479.
25. Huibregtse JM, Scheffner M, Beaudenon S, Howley PM. A family of proteins structurally and functionally related to the E6-AP ubiquitin-protein ligase. Proc Natl Acad Sci USA 1995;92:5249.
26. Ying SX, Hussain ZJ, Zhang YE. Smurf1 facilitates myogenic differentiation and antagonizes the bone morphogenetic protein-2-induced osteoblast conversion by targeting Smad5 for degradation. J Biol Chem 2003;278:39029–39036.
27. Sapkota G, Alarcon C, Spagnoli FM, Brivanlou AH, Massague J. Balancing BMP signaling through integrated inputs into the Smad1 linker. Mol Cell 2007;25:441–454.
28. Jackson MD, Fjeld CC, Denu JM. Probing the function of conserved residues in the serine/threonine phosphatase PP2Cα. Biochemistry 2003;42:8513–8521.
29. Chacko BM, Qin B, Correia JJ, Lam SS, de Caestecker MP, Lin K. The L3 loop and C-terminal phosphorylation jointly define Smad protein trimerization. Nat Struct Biol 2001;8:248–253.
30. Knockaert M, Sapkota G, Alarcon C, Massague J, Brivanlou AH. Unique players in the BMP pathway: small C-terminal domain phosphatases dephosphorylate Smad1 to attenuate BMP signaling. Proc Natl Acad Sci USA 2006;103:11940–11945.
31. Pera EM, Ikeda A, Eivers E, De Robertis EM. Integration of IGF, FGF, and anti-BMP signals via Smad1 phosphorylation in neural induction. Genes Dev 2003;17:3023–3028.
32. Kretzschmar M, Doody J, Massague J. Opposing BMP and EGF signalling pathways converge on the TGF-β family mediator Smad1. Nature 1997;389:618–622.
33. Fukuda T, Kanomata K, Nojima J, et al. A unique mutation of ALK2, G356D, found in a patient with fibrodysplasia ossificans progressiva is a moderately activated BMP type I receptor. Biochem Biophys Res Commun 2008;377:905–909.

Id4, a New Candidate Gene for Senile Osteoporosis, Acts as a Molecular Switch Promoting Osteoblast Differentiation

Yoshimi Tokuzawa[1☯], Ken Yagi[1☯], Yzumi Yamashita[1], Yutaka Nakachi[1], Itoshi Nikaido[1], Hidemasa Bono[1], Yuichi Ninomiya[1], Yukiko Kanesaki-Yatsuka[1], Masumi Akita[2], Hiromi Motegi[3], Shigeharu Wakana[3], Tetsuo Noda[3,4], Fred Sablitzky[5], Shigeki Arai[6], Riki Kurokawa[6], Toru Fukuda[7], Takenobu Katagiri[7], Christian Schönbach[8,9], Tatsuo Suda[1], Yosuke Mizuno[1], Yasushi Okazaki[1]*

1 Division of Functional Genomics and Systems Medicine, Research Center for Genomic Medicine, Saitama Medical University, Hidaka, Saitama, Japan, **2** Division of Morphological Science, Biomedical Research Center, Saitama Medical University, Iruma-gun, Saitama, Japan, **3** RIKEN BioResource Center, Tsukuba, Ibaraki, Japan, **4** The Cancer Institute of the Japanese Foundation for Cancer Research, Koto-ward, Tokyo, Japan, **5** Developmental Genetics and Gene Control, Institute of Genetics, University of Nottingham, Queen's Medical Center, Nottingham, United Kingdom, **6** Division of Gene Structure and Function, Research Center for Genomic Medicine, Saitama Medical University, Hidaka, Saitama, Japan, **7** Division of Pathophysiology, Research Center for Genomic Medicine, Saitama Medical University, Hidaka, Saitama, Japan, **8** Division of Genomics and Genetics, Nanyang Technological University School of Biological Sciences, Singapore, Singapore, **9** Department of Bioscience and Bioinformatics, Kyushu Institute of Technology, Iizuka, Fukuoka, Japan

Abstract

Excessive accumulation of bone marrow adipocytes observed in senile osteoporosis or age-related osteopenia is caused by the unbalanced differentiation of MSCs into bone marrow adipocytes or osteoblasts. Several transcription factors are known to regulate the balance between adipocyte and osteoblast differentiation. However, the molecular mechanisms that regulate the balance between adipocyte and osteoblast differentiation in the bone marrow have yet to be elucidated. To identify candidate genes associated with senile osteoporosis, we performed genome-wide expression analyses of differentiating osteoblasts and adipocytes. Among transcription factors that were enriched in the early phase of differentiation, Id4 was identified as a key molecule affecting the differentiation of both cell types. Experiments using bone marrow-derived stromal cell line ST2 and *Id4*-deficient mice showed that lack of *Id4* drastically reduces osteoblast differentiation and drives differentiation toward adipocytes. On the other hand knockdown of *Id4* in adipogenic-induced ST2 cells increased the expression of *Pparγ2*, a master regulator of adipocyte differentiation. Similar results were observed in bone marrow cells of femur and tibia of *Id4*-deficient mice. However the effect of *Id4* on *Pparγ2* and adipocyte differentiation is unlikely to be of direct nature. The mechanism of Id4 promoting osteoblast differentiation is associated with the Id4-mediated release of Hes1 from Hes1-Hey2 complexes. Hes1 increases the stability and transcriptional activity of Runx2, a key molecule of osteoblast differentiation, which results in an enhanced osteoblast-specific gene expression. The new role of Id4 in promoting osteoblast differentiation renders it a target for preventing the onset of senile osteoporosis.

Citation: Tokuzawa Y, Yagi K, Yamashita Y, Nakachi Y, Nikaido I, et al. (2010) Id4, a New Candidate Gene for Senile Osteoporosis, Acts as a Molecular Switch Promoting Osteoblast Differentiation. PLoS Genet 6(7): e1001019. doi:10.1371/journal.pgen.1001019

Editor: Gregory S. Barsh, Stanford University School of Medicine, United States of America

Received January 27, 2010; **Accepted** June 4, 2010; **Published** July 8, 2010

Funding: This work was supported by grants-in-aid of the Genome Network Project and Support Project of Strategic Research Center in Private Universities from the Ministry of Education, Culture, Sports, Science, and Technology (MEXT) to Saitama Medical University Research Center for Genomic Medicine. The funders had no role in study design, data collection and analysis, design, data collection and analysis, decision to publish, or preparation of the manuscript.

Competing Interests: The authors have declared that no competing interests exist.

* E-mail: okazaki@saitama-med.ac.jp

☯ These authors contributed equally to this work.

Introduction

Senile osteoporosis or age-related osteopenia is accompanied by increased bone marrow tissue adiposity [1]. Bone marrow adipocytes and osteoblasts are thought to originate from common mesenchymal stem cells (MSCs). Therefore, it has been suggested that the excessive accumulation of marrow adipocytes following bone loss is caused by unbalanced differentiation of MSCs into marrow adipocytes and osteoblasts [2]. Support for this hypothesis comes from studies of *peroxisome proliferators-activated receptor-γ* (*Pparγ*), a master regulator of adipocyte differentiation, deficient embryonic stem cells that showed an increase in osteoblast differentiation [3]. In contrast, calvarial adipocyte differentiation is augmented when *runt-related transcription factor 2 (Runx2)*, a master regulator of osteoblast differentiation has been knocked out [4]. Transcription factors Runx2 and *Sp7 transcription factor 7* (*Sp7*) regulate MSC commitment to osteoblast differentiation along with bone morphogenetic protein (BMP) signaling pathway [5]. Conversely, Pparγ and CCAAT/enhancer binding protein (C/EBP) transcription factor family members drive MSCs differentiation toward adipocytes [6]. Other proteins that regulate the balance between adipocyte and osteoblast differentiation are tafazzin, Wnt5a, Wnt10b, Msx2, C/EBPβ and basic helix-loop-helix (bHLH) family member e40 (Bhlhe40) [6–8]. Aforementioned transcription factors suppress adipocyte differentiation and promote osteoblast differentiation. Regardless of

Author Summary

Increased bone marrow adiposity is observed in the bone marrow of senile osteoporosis patients. This is caused by unbalanced differentiation of mesenchymal stem cells (MSCs) into osteoblast or adipocyte. Previous reports have indicated that several transcription factors play important roles in determining the direction of MSCs differentiation into osteoblast or adipocyte. So far, little is known about the overall dynamics and regulation of transcription factor expression changes leading to the imbalance of osteoblast and adipocyte differentiation inside the bone marrow. We have performed genome-wide gene expression analyses during the differentiation of MSCs into osteoblast or adipocyte. We identified basic helix-loop-helix transcription factor family member Id4 as a leading candidate controlling the differentiation toward adipocyte or osteoblast. Suppression of Id4 expression in MSCs repressed osteoblast differentiation and increased adipocyte differentiation. In contrast, overexpression of Id4 in MSCs promoted osteoblast differentiation and attenuated adipocyte differentiation. Moreover, *Id4*-mutant mice showed abnormal accumulation of lipid droplets in bone marrow and impaired bone formation activity. In summary, we have demonstrated a molecular function of Id4 in osteoblast differentiation. The findings revealed that Id4 is a molecular switch enhancing osteoblast differentiation at the expense of adipocyte differentiation.

these studies, the precise molecular mechanisms that regulate the balance between osteoblast and adipocyte differentiation in the bone marrow has yet to be elucidated. Hence, we aimed to identify transcription factors that regulate the direction of differentiation toward osteoblast or adipocyte by analyzing their genome-wide expression profiles in differentiation time series experiments.

We noticed in early phases a subgroup of transcription factors that appeared to function in both osteoblasts and adipocytes differentiation. Particularly, bHLH superfamily transcription factors were significantly enriched and up-regulated in the early phase of osteoblast differentiation.

The bHLH superfamily comprises transcription factors that form homo- or heterodimers and typically bind to a consensus sequence (CANNTG) called an E-box [9]. It is well known that bHLH transcription factors play important roles in development and cell differentiation. For example, Myod1 is a key differentiation factor of myoblasts and Srebf1 is involved in adipocyte differentiation [10,11]. Hairy and enhancer of split (Hes) family members of bHLH superfamily are crucial regulators of cortical development [12].

Here, we have identified Inhibitor of DNA binding 4 (Id4), which also belongs to the bHLH superfamily as a key molecule that regulates the direction of differentiation toward osteoblast or adipocyte *in vitro* and *in vivo* using genome wide expression study. Furthermore, we established that Id4 promotes osteoblast differentiation by enhancing Runx2 transcriptional activity through stabilization of Runx2 protein. The new role of Id4 in directing osteogenic and adipogenic cell fate makes it a likely target for preventing the onset of senile osteoporosis.

Results

Genome-wide expression profile predicts *Id4* as a candidate molecular switch in osteoblast and adipocyte differentiation

To delineate the sequential changes of transcription factors activating and repressing downstream osteogenic and/or adipogenic target genes, we evaluated the differentiation capability toward both osteoblasts and adipocytes using six cell lines (ST2, C2C12, DFAT-D1, PA6, 10T1/2, NRG). Of these, bone marrow-derived stromal cell line ST2 differentiated most efficiently into both osteoblasts and adipocytes (data not shown). Using Affymetrix mouse GeneChip, we aimed to identify clusters of transcription factors that are temporally co-regulated in one but not in another cluster (CIBEX Accession number: CBX90). Of 1,270 transcription factors, 407 genes were significantly up- or down- regulated in either osteoblast or adipocyte differentiation compared to the non-induced control (Table 1 and Table S1). Hierarchical clustering analysis of transcription factor gene expression data at 15 osteoblast and seven adipocyte differentiation time points (Figure 1A) revealed distinct clusters that represent phases of sequentially expressed transcription factors (Figure 1B). Differentiation into osteoblasts is characterized by five phases (Figure S1) whereas adipocyte differentiation resulted in four phases (Table S1). The early phases of osteoblast (1 hr) and adipocyte (48 hr) differentiation showed the greatest variability in transcription factor expression levels (Figure 2A and Table S1).

Chi-square testing for over-representation of transcription factors in each differentiation phase supported only six up-regulated bHLH superfamily members (*Id1*, *Id2*, *Npas4*, *Id4*, *Hes1* and *Bhlhe40*) of the immediate early phase osteoblast differentiation (1 hr) as significantly ($p<0.01$) enriched (Figure 2B). Since *Id4*, *Hes1* and *Bhlhe40* expression increased (decreased) twofold or greater during osteoblast (adipocyte) differentiation compared to the control (Figure 2C and Table 2), these transcription factors are likely to play a pivotal role in the regulation of osteoblast and adipocyte differentiation.

Indeed, Hes1 and Bhlhe40 are known to be involved in both differentiation pathways [8,13,14], whereas Id4 has not yet been implicated in either differentiation pathways. Additionally, *Id4* expression patterns in osteoblast and adipocyte differentiation were also compared by quantitative real-time PCR (qRT-PCR). Expression of *Id4* significantly increased during osteoblast differentiation, attained a peak on day 4 and decreased thereafter (Figure S2A). In contrast, *Id4* expression decreased during adipocyte differentiation (Figure S2B). Expression levels of *Id1* and *Id2* were also up-regulated in the early stage (1 hr) of osteoblast differentiation, but thereafter their expression dropped

Table 1. Expression behavior of 1,270 transcription factors selected from all mouse genes (Ensembl release 52) based on GO IDs (Table 3) during osteoblast and adipocyte differentiation.

Transcription Factors		Osteoblast Differentiation				
		↑	↓	↑↓	≈	Total
Adipocyte Differentiation	↑	22	6	4	70	102
	↓	25	40	21	132	218
	↑↓	3	5	2	2	12
	≈	42	26	7	863	938
	Total	92	77	34	1,067	1,270

Arrows indicate up- (↑), down-regulated (↓), or up- and down-regulated (↑↓) transcription factors. No change in expression is symbolized by the almost equal sign (≈).

doi:10.1371/journal.pgen.1001019.t001

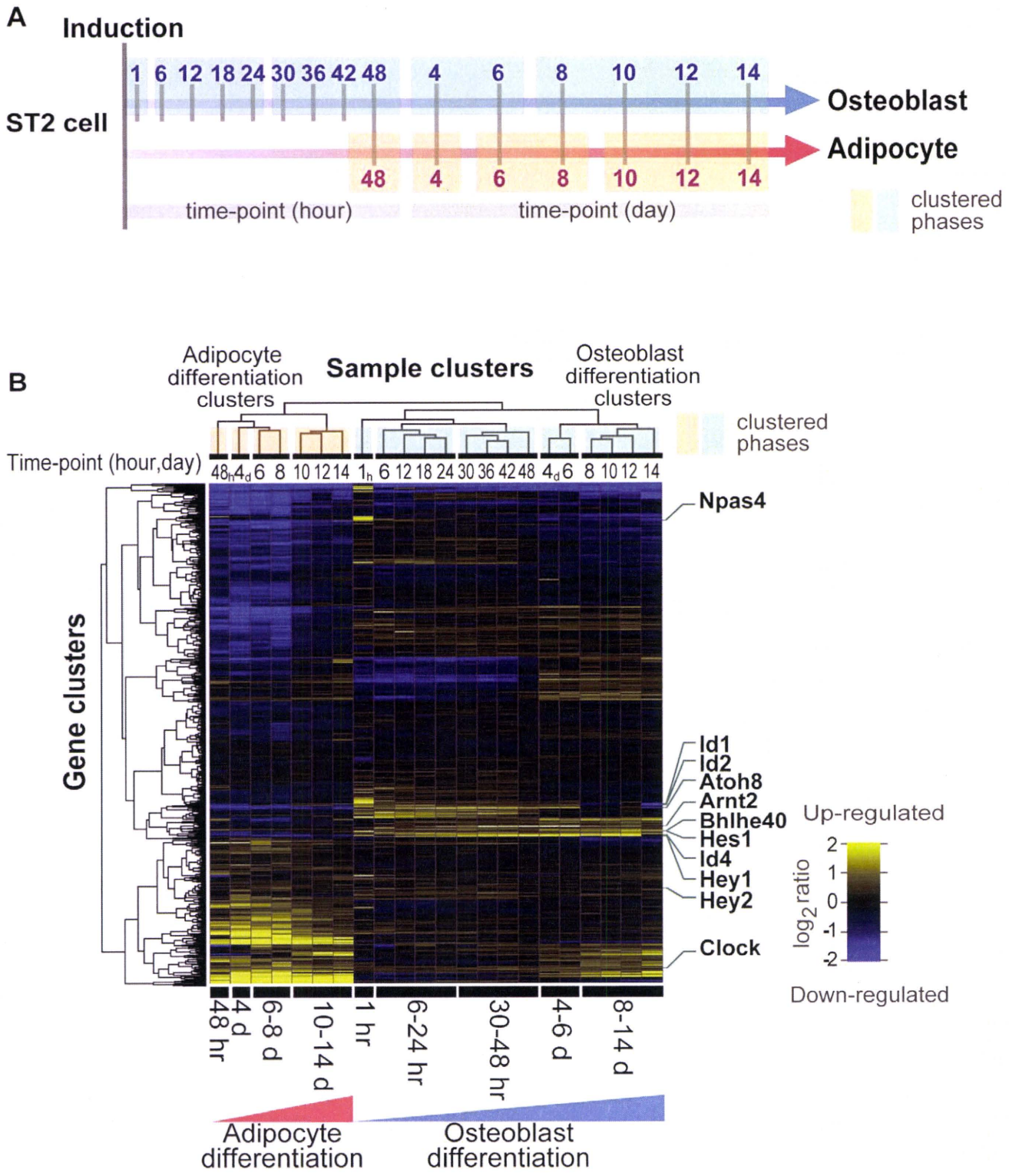

Figure 1. Transcription factor gene expression framework of differentiating ST2 cells. (A) Time-course sampling for gene expression analyses in ST2 cells. Vertical bars crossing the gradated blue and orange arrows indicate the sampling times during osteoblast and adipocyte differentiation, respectively. Five blue (osteoblasts) and four orange (adipocytes) boxes indicate the hierarchical clustering-derived phases of differentiation. (B) Gene expression heat map and clustering results of 1,270 transcription factors in 22 time-course samples.
doi:10.1371/journal.pgen.1001019.g001

to base levels (Figure 2C, upper panel). Therefore, we hypothesized that Id4 may act as a novel molecular switch in osteoblast and adipocyte differentiation.

Aside from *Id4*, *Hes1* and *Bhlhe40*, we identified additional bHLH members and various hypothetical and non-bHLH transcription factors as phase-specific candidate regulators of

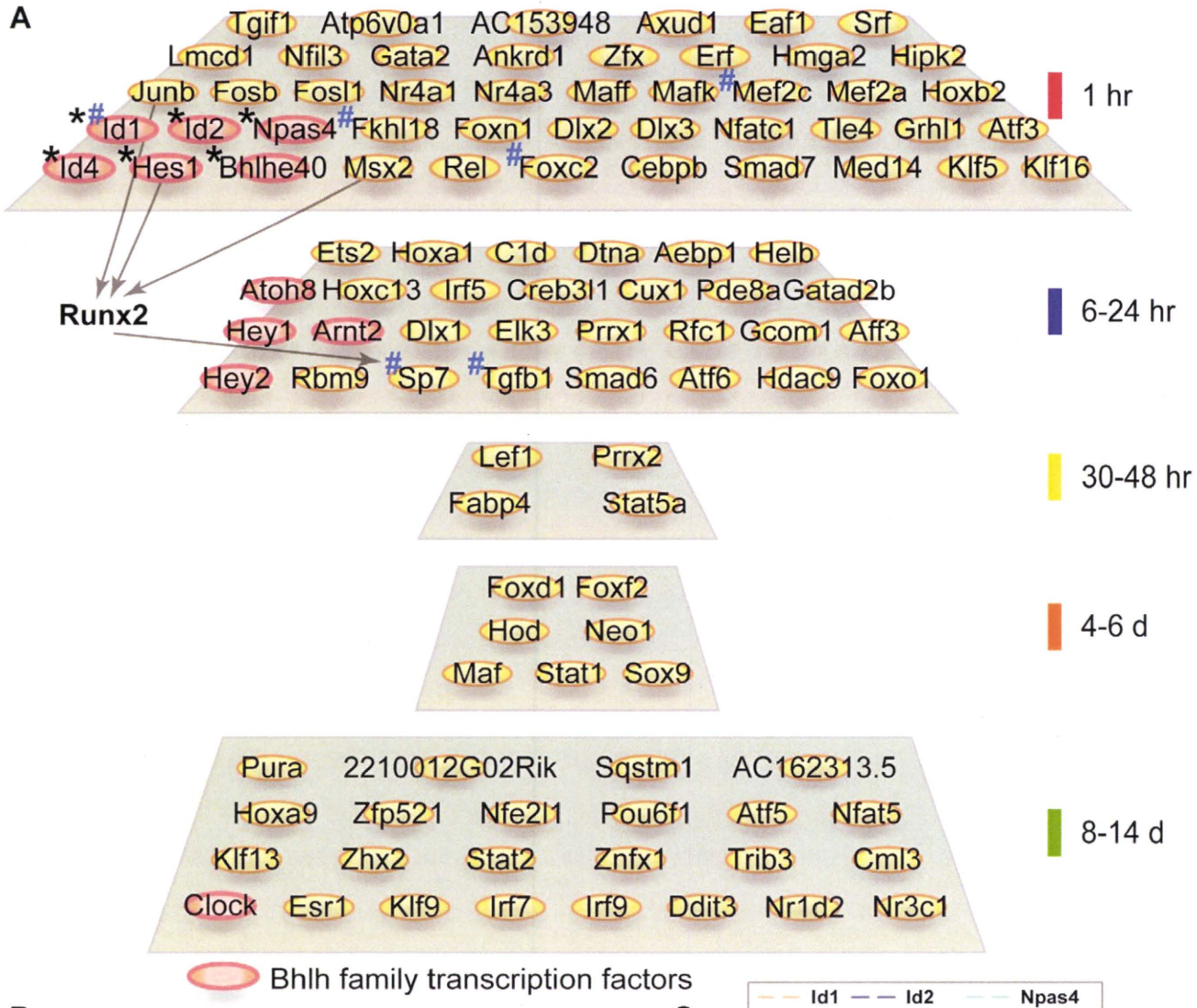

B

Observerd	Up-regulated at time point 1h	All genes other than up-regulated ones at 1h	Total no.
Bhlh family	6	106	112
All other genes	249	19,039	19,288
Total no.	255	19,145	19,400

Expected	Up-regulated at time point 1h	All genes other than up-regulated ones at 1h	Total no.
Bhlh family	1.47	110.53	112
All other genes	253.53	19,034.47	19,288
Total no.	255	19,145	19,400

C

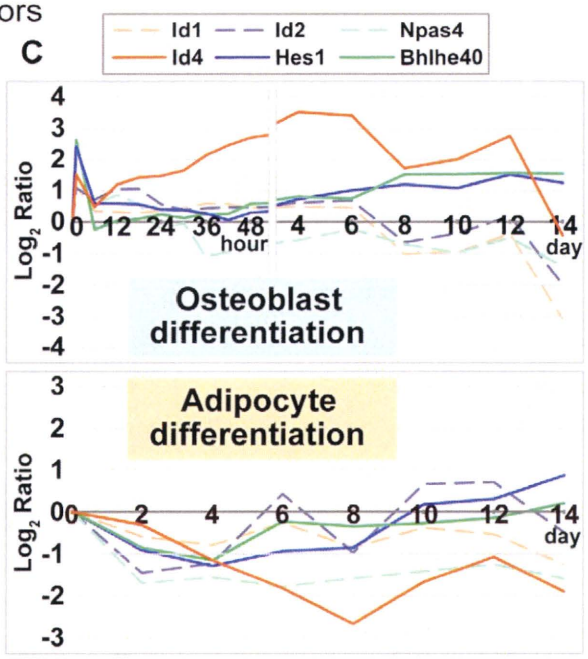

Figure 2. Enrichment of bHLH family in early phase of osteoblast differentiation and their expression pattern. (A) Summary of up-regulated transcription factors (Figure S1) associated with five phases of osteoblast differentiation. Asterisk (*): bHLH transcription factors that are overrepresented only during the early phase of osteoblast differentiation ($p<0.01$, Figure 2B). Sharp (#): transcription factors known to be associated with osteoblast differentiation and/or bone development. (B) Chi-square (χ^2) test for independence of bHLH superfamily genes in the immediate early phase (1 hr) of osteoblast differentiation. Null hypothesis: the occurrence of up-regulated bHLH transcription factors observed during the immediate early phase of osteoblast differentiation among all genes associated with probe set of Affymetrix GeneChip Mouse Genome 430 2.0 array is independent. Results of the contingency table (2×2 cells, degree of freedom = 1) allowed to reject the Null hypothesis. The expression of bHLH transcription factors was significantly up-regulated during the immediate early phase of osteoblast differentiation ($p<0.01$). (C) Expression pattern of six bHLH family genes in osteoblast and adipocyte differentiation. The chart represents expression changes of six bHLH genes during osteoblast and adipocyte differentiation. The horizontal axis indicates each time point after induction. The vertical axis indicates the logarithmic expression ratio (base 2) of each time point in comparison to the control (0 day).
doi:10.1371/journal.pgen.1001019.g002

osteo- and adipogenesis (Figure 2A and Table S1). The genes listed in Table S1 await further functional characterization regarding their involvement in osteoblast and/or adipocyte differentiation.

Id4 knockdown suppresses osteoblast differentiation of MSCs, and overexpression promotes osteoblast differentiation

To evaluate the potential role of Id4 in ST2 osteoblast differentiation, Id4 was suppressed by siRNA knockdown. As shown in Figure 3A, *Id4* siRNA (si*Id4*)-treated ST2 cells differentiating into osteoblasts showed a significant decrease in Id4 expression. The decline of *Id4* expression was accompanied by weak alkaline phosphatase (ALP) activity and reduced *bone γ carboxyglutamate protein 1* (*Bglap1* also called *osteocalcin*) expression (Figure 3B and 3C). Since both are markers of osteoblast differentiation, it appeared that Id4 is important in osteoblast differentiation of MSCs. We next evaluated whether forced expression of Id4 can promote osteoblast differentiation in MSCs by retroviral systems (Figure 3D). ST2 cells infected with Id4 recombinant retrovirus showed increased expression levels of *ALP* and *Bglap1* compared to cells infected with control virus independent of the presence or absence of BMP4 (Figure 3E and 3F). Taken together, Id4 promotes osteoblast differentiation of MSCs.

Id4 knockdown stimulates adipocyte differentiation, and overexpression attenuates lipid accumulation

Id4 knockdown in adipogenesis-induced ST2 cells (Figure 4A) significantly increased expression levels of other adipogenic marker genes such as *Pparγ2* [15] and *Adipoq* [16] (Figure 4B and 4C). Concomitantly, the number of Oil Red O stained lipid droplets and triglyceride levels also increased (Figure 4D and 4E). Forced expression of Id4 was confirmed by transfection into Cos7 cells with Id4 expression vector (Figure 4F). Adipocytes differentiated from ST2 cells transfected with Id4 expression vector showed slightly but significantly decreased lipid accumulation compared to empty vector transfectants (Figure 4G). The combined results of *Id4* siRNA knockdown and overexpression in ST2 suggest that Id4 attenuates differentiation of MSCs into adipocytes.

Id4-knockout mice ($Id4^{-/-}$) showed impaired osteoblast differentiation

Previously $Id4^{-/-}$ mice were studied only in context of neural development [17]. We confirmed that *Id4* expression was highest in the brain followed by cortical bone, kidney, thymus and bone marrow of C57BL/6J mice (Figure 5A). The body length and weight of 4 weeks old $Id4^{-/-}$ mice was 13–15% shorter and 35–40% lower compared to wild-type ($Id4^{+/+}$) littermates (Figure 5B and 5C). $Id4^{-/-}$ mice showed severe growth retardation and died by 5 weeks. In addition, we observed visible skeletal phenotypes of $Id4^{-/-}$ mice, but no skeletal deformities (data not shown). Altogether, our data hint at an important role of Id4 in bone formation.

Bone histological analysis of $Id4^{-/-}$ mice revealed significantly decreased bone volume (BV) in the 6th lumbar (Figure 5D and 5E).

Table 2. Expression of eleven bHLH transcription factors shown in Figure 2A.

	Differentiation		Differentiation Clusters	
Gene Symbol	**Osteoblast**	**Adipocyte**	**Osteoblast**	**Adipocyte**
Bhlhe40	↑	↓	1h ↑	4d ↓
Hes1	↑	↓	1h ↑	4d ↓
Id1	↑ ↓	↓	1h ↑	10d–14d ↓
Id2	↑ ↓	↓	1h ↑	2d ↓
Id4	↑	↓	1h ↑	4d ↓
Npas4	↑ ↓	↓	1h ↑	2d ↓
Arnt2	↑	≈	6h–24h ↑	≈
Atoh8	↑ ↓	↓	6h–24h ↑	2d ↓
Hey1	↑	≈	6h–24h ↑	≈
Hey2	↑	≈	6h–24h ↑	≈
Clock	↑	↑	8d–14d ↑	10d–14d ↑

Of eleven transcription factors, *Bhlhe40*, *Hes1* and *Id4* were two-fold or greater up-regulated during osteoblast differentiation. On the other hand, these genes were one-half fold or greater down-regulated during adipocyte differentiation. Arrows indicate up- (↑), down-regulated (↓), or up- and downregulated (↑ ↓) bHLH genes. No change in expression is symbolized by the almost equal sign (≈). Crosstalk functions between osteoblast and adipocyte differentiation have been reported for Bhlhe40 [8], Hes1 [13,14] and Id4 (this study), only.
doi:10.1371/journal.pgen.1001019.t002

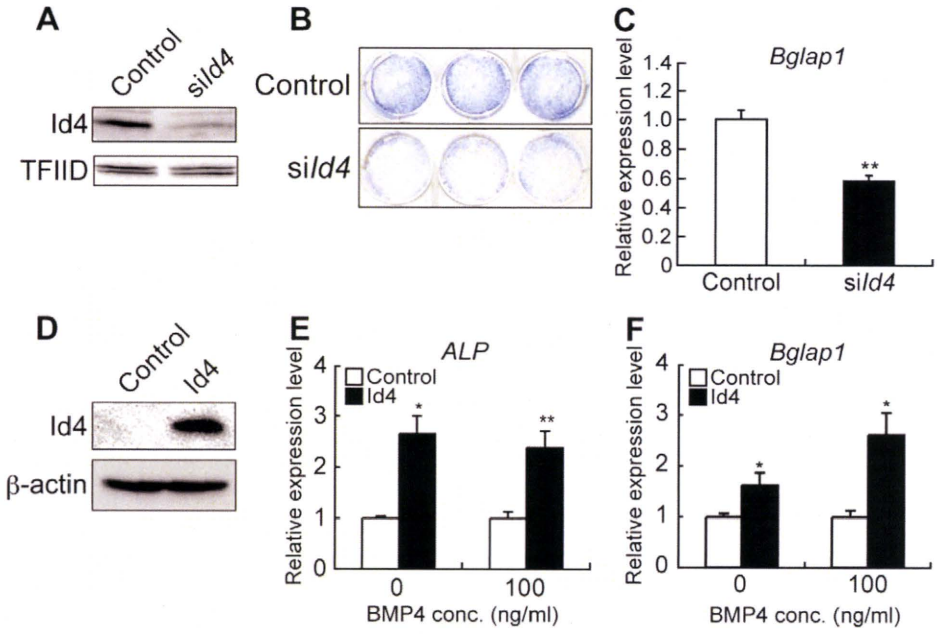

Figure 3. *Id4* promotes osteoblast differentiation in ST2 cells. (A) Western blotting of anti-Id4 antibody using ST2 nuclear extract. TFIID was detected as a loading control. Specific reduction of Id4 expression at day 2 after induction of ST2 cells treated with *Id4* siRNA (si*Id4*) for osteoblast differentiation. (B,C) Decrease in ALP activity (B) and *Bglap1* expression (C) at day 6 after induction of osteoblast differentiation in ST2 cells treated with si*Id4* as compared to the negative control. (D) Western blotting of anti-Id4 antibody using ST2 cell lysate, infected with Id4 retrovirus or control retrovirus (control). β-actin was detected as a loading control. (E,F) Increase in *ALP* (E) and *Bglap1* (F) expression at day 4 after infection with *Id4* virus as compared to the control virus in non-induced ST2 and ST2 osteoblast. Relative expression levels of *ALP* and *Bglap1* mRNA were measured by qRT-PCR. qRT-PCR data were subjected to Student's t-tests. Each error bar represents the mean ± SE of triplicates. *$p<0.05$ versus control, **$p<0.01$ versus control.

doi:10.1371/journal.pgen.1001019.g003

The bone formation rate (BFR) was decreased in $Id4^{-/-}$ mice compared to $Id4^{+/+}$ mice (Figure 5F and 5G). The BV to total volume ratio, BFR to bone surface (BS) ratio and mineral apposition rate (MAR) of $Id4^{-/-}$ mice were 57.3%, 28.1% and 30.7% lower compared to $Id4^{+/+}$ mice in the 6th lumbar, respectively (Figure 5N–5P).

In $Id4^{+/+}$ mice, active cuboidal-shaped osteoblasts (type II osteoblasts) were distributed in a row along the lumbar BS (Figure 5H), whereas in the corresponding region of $Id4^{-/-}$ mice osteoblasts were predominantly flat and resting (type IV osteoblasts; lining cells) (Figure 5I). The number of osteoblasts as a whole did not change significantly between $Id4^{+/+}$ and $Id4^{-/-}$ mice (data not shown). However, in $Id4^{-/-}$ mice the population of active osteoblasts was reduced (type II, Figure 5Q), whereas inactive osteoblasts accumulated (type IV, Figure 5R). These findings imply that Id4 modulates both differentiation of osteoblasts from pre-osteoblasts and regulation of osteoblast maturation.

Impaired bone formation was also observed in the lateral calvaria of $Id4^{-/-}$ mice (Figure 5K and 5M). In wild type mice, osteoblasts were closely lined up along the calvarial BS (Figure 5J). In contrast, no osteoblasts were observed along the calvarial bone of $Id4^{-/-}$ mice (Figure 5K). The osteoid thickness, BFR to BS ratios and MAR of $Id4^{-/-}$ mice calvarial bones were 61.5%, 49.1% and 65.2% of $Id4^{+/+}$ mice, respectively (Figure 5S, 5O, and 5P). These results suggest that Id4 is important for both endochondorial and membranous ossification. Growth Plate Width and Longitudinal Growth Rate (Lo. G. R) of $Id4^{-/-}$ mice tibia were 68.4% and 57.1% of $Id4^{+/+}$ mice, respectively (Figure S3A, S3B, S3C, S3D), which may have caused the growth retardation of $Id4^{-/-}$ mice.

Id4 interacts with Hey2 and inhibits the transcriptional repression of Hey2

Id family members are known to heterodimerize with other bHLH transcriptional factors, thus inhibiting the binding to the E-box motif [18]. To explore whether heterodimerized Id4 switches the direction of osteoblast and adipocyte differentiation, we assayed Id4 protein-protein interactions and analyzed their effects. Using immunoprecipitation we attempted to capture for candidate bHLH transcription factors that bind to Id4. Out of four tested bHLH transcription factors (Hes1, hairy/enhancer-of-split related with YRPW motif 1; Hey1, hairy/enhancer-of-split related with YRPW motif 2; Hey2 and Bhlhe40) (Figure S4A), only Hey2 bound to Id4 (Figure 6A, Figure S4A and S4B). An earlier study demonstrated that Hey2 is forming heterodimers with Hes1, which then bind to the E-box motif and repress transcription [19]. Therefore, we tested the effect of Id4 on transcriptional repression of Hey2/Hes1 heterodimers against the E-box element. Transcriptional repression onto E-box element in the presence of either Hey2 or Hes1 showed no effect or 39% inhibition of E-box transcriptional activity relative to control (empty expression vector), respectively (Figure 6B). Although luciferase activity was lowest in the presence of both Hey2 and Hes1, inhibition of transcriptional repression by Id4 increased in dose-dependent manner (Figure 6B). We also demonstrated that Hey2-Hes1 binding was abrogated with the dose-dependent increase of Id4 (Figure 6C, lane 5 and lane 6). Taken together, we confirmed that Id4 reverses the transcriptional repression by Hey2-Hes1 heterodimer in a dose-dependent manner.

Id4/Hey2 complex indirectly enhances Runx2 transcriptional activity

The presence of inactive osteoblasts (Figure 5I and 5R) in the bone tissues of the $Id4^{-/-}$ mice let us assume that Id4 may affect

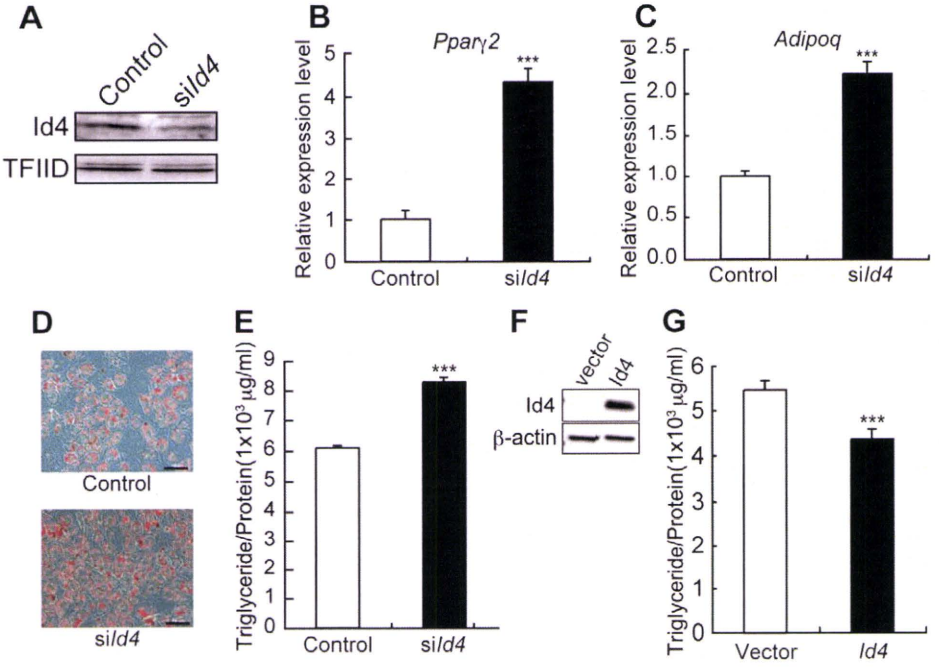

Figure 4. *Id4* weakly suppresses adipocyte differentiation in ST2 cells. (A) Western blotting of anti-Id4 antibody using ST2 nuclear extract. TFIID was detected as a loading control. Specific reduction of Id4 expression at day 2 after induction of ST2 cells treated with si*Id4* for adipocyte differentiation. (B,C) Increase in *Pparγ2* (B) and *Adipoq* (C) expression at day 1 after induction of adipocyte differentiation and treatment with si*Id4*. Relative expression levels of *Pparγ2* and *Adipoq* mRNA were measured by qRT-PCR. (D) Oil Red O staining of ST2 cells at day 4 after induction of adipocyte differentiation in presence of control or si*Id4*. Original magnification: ×200; bar = 100 μm. (E) Lipid content of ST2 cells measured as triglyceride level at day 5 after adipogenic induction in presence of control or si*Id4*. (F) Western blotting of anti-Id4 antibody using Cos7 cell lysate, transfected with Id4 expression vector or empty vector (Vector) as a control. β-actin was detected as a loading control. (G) Lipid content of ST2 cells transfected with Id4 expression vector or empty vector measured as triglyceride level at day 5 after adipogenic induction. qRT-PCR and lipid content data were subjected to Student's t-tests. Each error bar represents the mean ± SE of triplicates. $*p<0.05$ versus control and $***p<0.005$ versus control.

doi:10.1371/journal.pgen.1001019.g004

the actions of Runx2 and Sp7, a key osteogenic differentiation molecule [20–22]. Osteoblast marker gene *Bglap1* expression level decreased not only in primary osteoblasts but also in embryonic day18.5 (E18.5) limb of $Id4^{-/-}$ mice (Figure S5A and S5B). *Bglap1*, a target gene of Runx2 has an E-box element other than osteoblast-specific element 2 (OSE2), which binds Runx2 to the promoter [23]. Therefore, we measured the promoter activity to examine the influence of Id4 on *Bglap1* E-box promoter-dependent transcriptional activity of Runx2. Although the suppression of *Bglap1* promoter activity by addition of Hes1 and Hey2 was not detected, a dose-dependent increase of transcriptional activity by Id4 was observed when testing the OSE2 element-containing promoter. When using the promoter without OSE2 the increase in transcriptional activity was not seen (Figure 7A). Since direct interaction between Id4 and Runx2 was ruled out experimentally (data not shown), Id4 may indirectly influence Runx2 transcriptional activity through Hes1. Hes1 is known to stimulate the transcriptional activity of Runx2 protein by increasing its stability during osteoblast differentiation [24]. We also confirmed that the addition of Hes1 stabilizes Runx2 protein. Interestingly, the addition of Id4 further increased the stabilization and accumulation of Runx2 (Figure 7B). Taken together, it appears that Id4 enhances Runx2 transcriptional activity through stabilization of Runx2 protein.

Taking into account the timing of the elevated *Id4* expression (Figure 2C and Figure S2A), our results strongly suggest that Id4 is indirectly driving the Hes1-mediated Runx2 stabilization during osteoblast differentiation. The facts that both Hes1 and Hey2 bind to the OSE2 element-containing *Bglap1* promoter region assessed by ChIP-qPCR, and that the amount of bound Hes1 and Hey2 decreased in ST2 osteoblasts (Figure 7C) further support this idea. However, the exact binding site of Hes1-Hey2 heterodimer remains to be identified. The proposed mechanism of Id4 action during osteoblast differentiation is illustrated in Figure 7D.

$Id4^{-/-}$ mice showed increased adipocytes

Id4 knockdown promoted adipocyte differentiation in ST2 cells (Figure 4B–4E). Histological analysis of $Id4^{-/-}$ tibia bones revealed elevated numbers of adipocytes in epiphyseal bone marrow of tibia compared to $Id4^{+/+}$ mice (Figure 8A–8D). The entire analyzed area of epiphyseal tibia bone marrow was occupied by adipocytes in $Id4^{-/-}$ mice (Figure 8E). Moreover, *Pparγ2* expression levels were also increased in bone marrow cells of femur and tibia of $Id4^{-/-}$ mice (Figure 8F). In comparison to $Id4^{+/+}$ mice, the number of adipocytes in the lateral calvaria was markedly increased in $Id4^{-/-}$ mice (Figure 5K). These aberrant traits observed in $Id4^{-/-}$ mice implicate Id4 as a crucial molecule in the lineage choice of MSCs differentiating into either osteoblasts or adipocytes (Figure 8G).

Discussion

In this study, we have delineated clusters of transcription factors that act as key regulators in the osteoblast and adipocyte differentiation network. The observation of sometimes disparately regulated transcription factors, led us to hypothesize a molecular

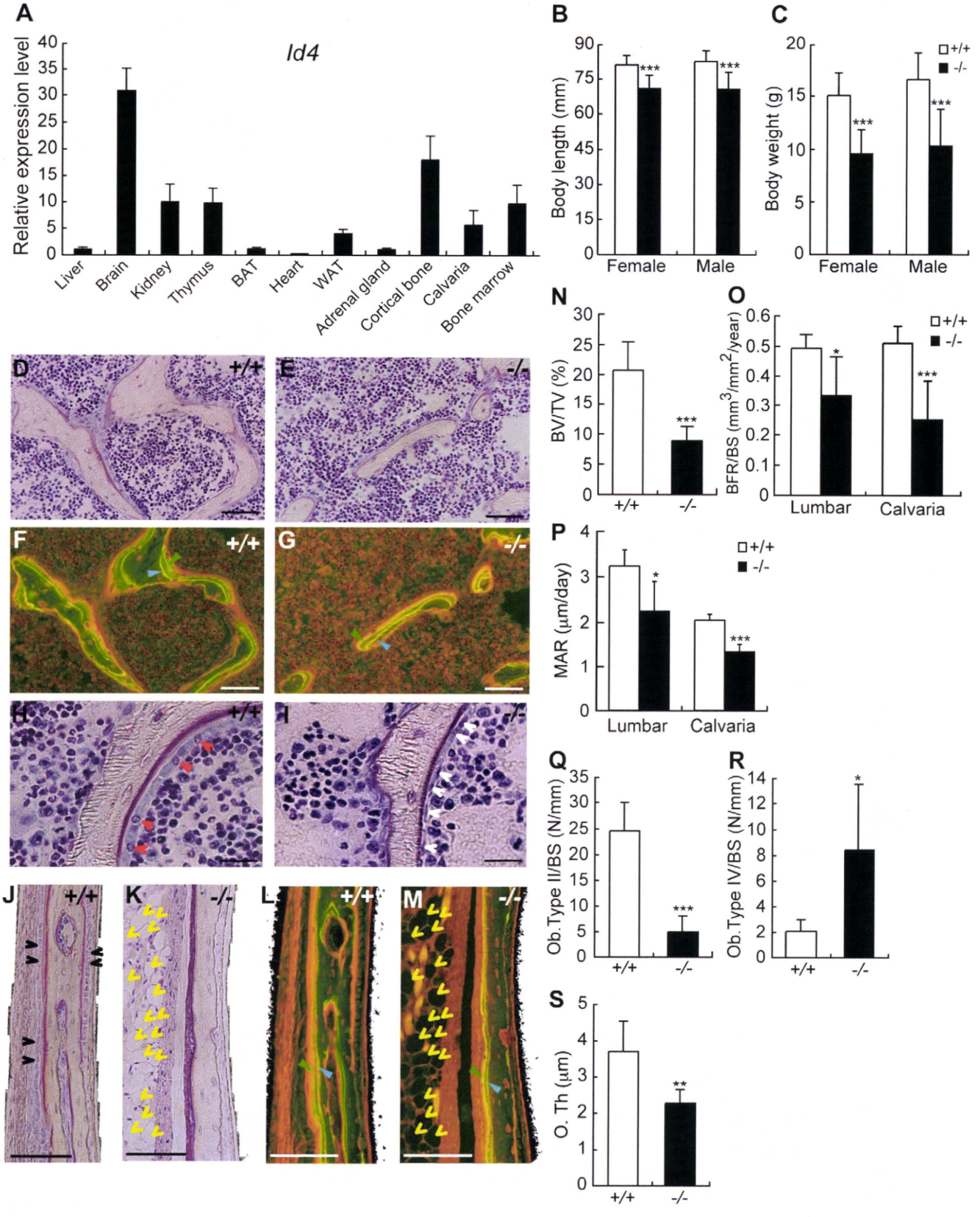

Figure 5. 4-week-old *Id4* knockout (*Id4*$^{-/-}$) mice show disturbance in growth and impaired osteoblast differentiation. (A) Tissue distribution of *Id4* mRNA in C57BL/6J male mice was measured by qRT-PCR. Brown adipose tissues; BAT, White adipose tissues; WAT. (B,C) Body length (B) and body weight (C) of wild-type (*Id4*$^{+/+}$) and *Id4*$^{-/-}$ mice. (D,E,H,I) Villanueva staining of the 6th lumbar bone of *Id4*$^{+/+}$ mice (D,H) and *Id4*$^{-/-}$ mice (E,I). Red and white arrowheads indicate active cuboidal-shaped osteoblasts (type II osteoblasts) and flattened resting osteoblasts (type IV